Check for updates

Exploration

REVIEW OPEN ACCESS

Plasma Activate Nitrogen for Efficient Ammonia Synthesis

Plasma Ammonia Synthesis

Yamei Zhang[1] | Jianfei Yu[1] | Haixia Wu[1] | Zhijun Zhao[2] | Hongjin Xia[3] | Qingyang Li[3] | Yiran Wang[4] | Dongyang Li[5] | Qian Wang[4]

[1]School of Chemical and Pharmaceutical Engineering, Hebei University of Science and Technology, Shijiazhuang, China | [2]College of New Materials and Chemical Engineering, Beijing Institute of Petrochemical Technology, Beijing, China | [3]Institute of Advanced Wear & Corrosion Resistant and Functional Materials, Jinan University, Guangzhou, China | [4]Institute of Process Engineering, Chinese Academy of Sciences, Beijing, China | [5]Department of Chemical and Materials Engineering, University of Alberta, Edmonton, Canada

Correspondence: Zhijun Zhao (zhaozj@tsinghua.org.cn) | Qingyang Li (qingyang@jnu.edu.cn) | Dongyang Li (dongyang.li@ualberta.ca) | Qian Wang (wangq@ipe.ac.cn)

Received: 20 January 2025 | **Revised:** 30 August 2025 | **Accepted:** 30 October 2025

Keywords: ammonia | catalysis | electrochemistry | energy conversion | nitrogen chemistry | plasma

ABSTRACT

Synthetic ammonia is of great significance to the development of industry and agriculture. At present, its manufacturing production is still dominated by century-old Haber–Bosch process, involving in huge amounts of energy consumptions and carbon dioxide emissions. Hence, it is of great significance to develop green and sustainable alternative technologies, such as photo-, thermo-, and electro-catalytic syntheses of ammonia. Nevertheless, the intrinsic inertness of nitrogen results in low ammonia yield of above candidates, which still cannot meet commercialization expectations. Recent researches have successfully demonstrated that plasma can effectively activate the decomposition of nitrogen and hydrogen under ambient conditions, thereby significantly improving the ammonia yield of these alternative strategies. This review systematically summarizes the classification and reaction mechanism of plasma for this reason, and discusses the synergy between different plasma and catalytic methods along with energy consumptions in detail. In the meantime, the future development trend is also forecasted.

1 | Introduction

Ammonia (NH_3) is an indispensable raw material for industrial and agricultural productions and meanwhile, it is an outstanding hydrogen (H_2) energy carrier with the advantages of high energy density (~4.25 kWh L^{-1}), convenient transportation and storage [1–5]. Up to now, the synthetic NH_3 industry is still dominated by the century-old Haber–Bosch (H-B) process (over 90% of annual global production), in which the reaction needs very harsh temperature (350–450°C) and pressure (100–200 bar) along with the catalysts [6], involving in large amounts of energy consumptions (1%–2% of the world's energy sources) as well as carbon dioxide emissions (~1.3%) [7]. Among them, most of the energy consumptions are spent on the dissociation of triple bond (N≡N), which is recognized as a critical step for deriving the nitrogen (N_2) reduction reaction (NRR, $N_2 + 3H_2 \rightarrow 2NH_3$) [8]. How to boost N_2 activation under mild conditions is therefore of great significance to energy conservation, emission reduction, and sustainable NH_3 synthesis.

N_2 is characterized by high bond dissociation enthalpy (941 kJ mol^{-1}), non-polarity, large ionization potential, negative electron

Yamei Zhang and Jianfei Yu contributed equally to this work.

This is an open access article under the terms of the Creative Commons Attribution License, which permits use, distribution and reproduction in any medium, provided the original work is properly cited.

© 2026 The Author(s). *Exploration* published by Henan University and John Wiley & Sons Australia, Ltd.

affinity energy, and broad gap between the lowest unoccupied molecular orbital and the highest occupied molecular orbital (~10.82 eV), and thus its activation is extremely difficult [9–11]. Although high temperature is conducive to the dissociation of N≡N bond and the desorption of intermediates on the catalyst surface, excessive temperatures are thermodynamically unfavorable toward NH_3 synthesis, because the NRR is essentially exothermic reaction ($\Delta H = 46.27$ kJ mol^{-1}). Obviously, raising the NRR temperature is in conflict with N_2 activation. This requires the exploration of more mild alternative technologies for realizing green and efficient N_2 activation, which is an urgent challenge to be met by synthetic NH_3 industry, currently [12, 13].

So far, both microelectronic and macroscopic fields have been demonstrated to be effective in activating N_2. For the microelectronic effect, it is mainly owing to the catalyst modification, for example, defect engineering, crystal facet tailoring, and hybrid strategy [14–20]. In this regard, scholars have devoted considerable efforts to activating N_2 through catalyst design [21]. For example, introducing defect (i.e., vacancy and heteroatom) into the catalyst at the atomic level can effectively manipulate its electronic structure, thereby improving the chemical affinity of catalytically active center to N_2. Tailoring the atomic arrangement of catalyst, including alloying, amorphization, crystal engineering and control, etc., may also significantly activate N_2. Besides, the producing hybrid catalyst through combined different components and structural heterogeneities is feasible method for enhancing the chemisorption and activation of N_2 [22–25]. As for the macroscopic effect, it mainly includes plasma, light and electric fields. Among them, the plasma field is used to trigger the discharge of N_2 molecules, thereby producing excited or substable species, and achieving their activation. The light field can excite the catalyst to generate photo-generated electrons, hot electrons, and photo-thermal effects, which may promote the adsorption and activation processes of N_2. The electric field usually possesses highly localized electron density along with beneficial polarization effect on the N_2, which boost the charge transfer from catalyst to N_2, thus significantly reducing the energy level in the lowest unoccupied molecular orbital of N_2. Although the catalyst can optimize the electronic structure of active sites through defect engineering and crystal surface regulation, etc., thereby promoting the N_2 affinity, the improvement effect is limited by its intrinsic properties. It is therefore difficult to achieve the efficient dissociation of N_2 under mild conditions. As for the light field, it majorly depends on the generation efficiency of photo-generated carriers. The polarization effect of electric field may also decrease the lowest orbital energy level of N_2, but its scope of work is highly localized. In contrast, the plasma-activated N_2 possesses relatively unique advantages, such as efficient energy transfer and mild reaction condition. Moreover, it circumvents the linear scaling relationship between the adsorption energy of nitrogen species and the dissociation energy of N_2 in conventional thermocatalysis, opening up new reaction pathways on the catalyst surface. It can also be coupled with electrical, optical, and thermal catalysis to form multi-field synergy, thereby realizing the energy consumption optimization. Recent advances in activation of N_2 with light field [26, 27], electric field [28–30], and plasma field [31–33], have been summarized by researchers in detail. However, most of them mainly focus on a single field [34–36], ignore the cascade design with other technologies, especially the synergistic effect of plasma and catalysis on the N_2 activation, and fail to quantitatively analyze their energy consumptions. This is the motivation for writing this review on the plasma activation of N_2 for efficient NH_3 synthesis. The review wants to put forward some suggestions for the future development direction of plasma-catalytic NH_3 synthesis, through systematically summarizing the current status at domestic and international researches. For instance, the influences of different plasmas and catalytic systems on the NH_3 synthesis are systematically summarized, and they are classified and analyzed in detail, aiming at the synergistic effect of plasma catalysis, as schematically illustrated in Figure 1.

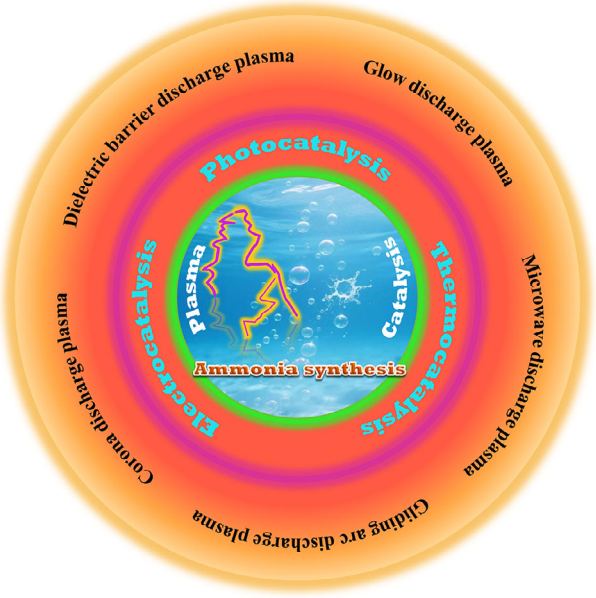


FIGURE 1 | Synergistic effect between plasma and catalysis on NH_3 synthesis.

2 | Plasma-Enhanced NH_3 Synthesis

2.1 | Plasma-Enhanced NH_3 Synthesis Processes

The characteristics of plasma are mainly determined by its primitive reactions, involving in the ionization, excitation and dissociation, composition, attachment and detachment.

1. Ionization: The process of neutral atoms or molecules losing electrons and forming cations is called ionization, which is the first and most central process in the plasma chemistry. Electrons first obtain energy under the action of electric field, and offer energy to other components, resulting in the ionization, excitation, dissociation and other plasma chemical processes, due to their low mass and high mobility. The ionization process can be mainly divided into direct electron collisional ionization, electron-collisional accumulated ionization, heavy-particle collisional ionization, photoionization, surface ionization and electron emission. The ground state electrons may separate from the atoms, thereby triggering the generation of a series of charged particles, through the ionization process.

27662098, 2026, 1, Downloaded from https://onlinelibrary.wiley.com/doi/10.1002/EXP.20240438 by CochraneChina, Wiley Online Library on [08/06/2026]. See the Terms and Conditions (https://onlinelibrary.wiley.com/terms-and-conditions) on Wiley Online Library for rules of use; OA articles are governed by the applicable Creative Commons License

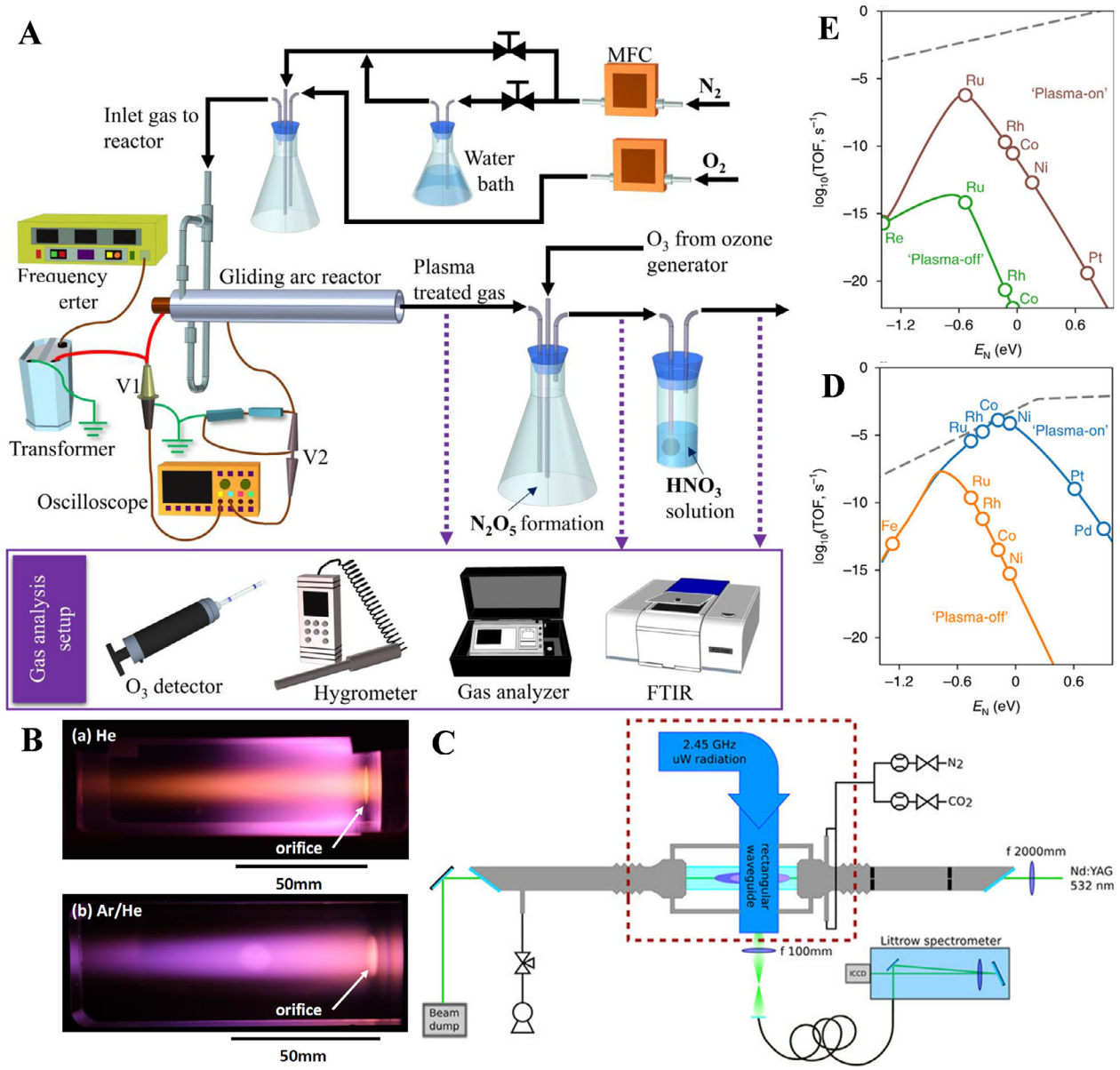


FIGURE 2 | (A) Schematic diagram of the GAD reactor. Reproduced with permission Ref. [38]. (B) Photographs of the He and Ar-based plasmas. Reproduced with permission Ref. [37]. (C) Schematic of the spontaneous Raman scattering setup installed at the flowing MW plasma reactor. Reproduced with permission Ref. [41]. (D) Comparison of N_2 vibrational-distribution-weighted and thermal NH_3 synthesis rates on the step, and (E) terrace sites, respectively. Reproduced with permission Ref. [42].

2. Excitation and dissociation: The high chemical activity of plasma is based on its super-equilibrium concentration of active particles, including excited state particles [37]. The collision between neutral particles and electrons causes electron transitions to form excited state particles. In this connection, Denra et al. [38]. studied the N_2 fixation in the plasma at surrounding conditions (Figure 2A), and proposed that there were three excitation modes, including rotational excitation, vibrational excitation, and electronic excitation. Among them, the excitation degree can be expressed by rotation, vibration, and electronic excitation temperature, while the electronic excitation temperature is comparable to electron temperature, and the gas temperature, ion temperature, and rotational temperature are also equal to each other [39]. However, the vibrational temperature may rise above the gas temperature in the plasma. The excitation process of plasma is often accompanied by the decomposition of substances and the generation of reactive molecules, so it plays a key role in the plasma chemical reaction and substance synthesis. The vibration excitation energy of N_2 is 0.29 eV, and the electronic excitation energy is 6.17 eV. Both of them are lower than the dissociation energy of N_2. At the same time, the vibration excitation has also a lower energy threshold, compared with that of electronic excitation energy. As a result, the vibration excitation may be the main excitation mode of N_2 in the atmospheric pressure plasma. And most of the electron-molecular exchange energy will be used for vibration excitation [40].

Yamazaki and Sasaki [37] comparatively investigated the vibrational temperature of N_2 in the downstream of helicon-wave

27662098, 2026, 1, Downloaded from https://onlinelibrary.wiley.com/doi/10.1002/EXP.20240438 by CochraneChina, Wiley Online Library on [08/06/2026]. See the Terms and Conditions (https://onlinelibrary.wiley.com/terms-and-conditions) on Wiley Online Library for rules of use; OA articles are governed by the applicable Creative Commons License

excited helium (He) and argon (Ar)-based plasmas, respectively. As shown in Figure 2B, the vibrational temperature in the He plasma is higher than that in the ionizing Ar/He plasma. In general, a higher vibrational temperature is more beneficial to boost the reactions powered by vibrational excited states. Gatti et al. [41]. also assessed the preferential vibrational excitation of N_2 in the MW plasma by Raman scattering (Figure 2C), and confirmed that the vibrational excitation is promising strategy for promoting the chemical reactivity of endothermic reactions. Moreover, Mehta et al. [42]. developed a micro-kinetic model incorporating the potential effects of vibrational excitation in N_2, based on the density functional theory (DFT) calculations reported in the literature, and proposed that the transition metals bound to N_2 were too weak to be catalytically active in the thermal reactions. The reaction rate can be increased more efficiently in the plasma catalytic reaction (Figure 2D), and the vibrational excitation of N_2 can increase the synthesis rate of NH_3 by reducing the dissociative adsorption energy (Figure 2E). These results provide an important guidance for optimizing catalysts of the plasma-assisted NH_3 synthesis. In addition to excitation, the collisions between electrons and neutral particles can lead to molecular dissociation, while the binding energy of the molecule-ion composition may also cause the intermediates to dissociate and excite the dissociated products.

1. Composition: The process of positive and negative charged particles produced by the ionization recombine into neutral particles is called composition, which can be divided into spatial and surface compositions, depending on the location where it occurs. The composition is regarded as the reverse process of ionization, and usually excites the composite product as well.
2. Attachment and detachment: The process of atoms or molecules adsorbing electrons to generate negative ions is called attachment. On the contrary, the process of desorbing electrons to produce atoms and molecules is called detachment. Understanding the above processes is very important to investigate the mechanism responsible for plasma-enhanced NH_3 synthesis.

2.2 | Plasma-Enhanced Mechanism

Understanding the mechanism of plasma-activated N_2 process is of great significance for enhancing the NH_3 synthesis. As illustrated in Figure 3A, the enhancement process involves two key stages, that is, the plasma activation of N_2 and H_2 to generate active species, followed by the combination of these active species to form NH_3. Specifically, the activation of N_2 and H_2 occurs within the plasma, producing active particles such as nitrogen molecule (N_2*), vibrationally excited state of nitrogen [N_2 (v)], nitrogen radical (N•), and hydrogen atom (H). These particles subsequently participate in catalytic reactions on the catalyst surface. The N_2* are excited to produce N_2 (v) through electron collisions. This process is primarily characterized by vibrational and electronic excitation. The plasma-activated N_2 (v) can then adsorb onto the catalyst surface, and dissociate into the N•. Similarly, the activation process of H_2 under plasma action is also the H_2 dissociates into H atoms. The active species are combined to synthesize NH_3 by a stepwise hydrogenation process of N_2. Among them, the NH• radicals are mainly generated through the combination of active nitrogen species and active hydrogen species on the catalyst surface. The NH• intermediates can further undergo hydrogenation with active hydrogen species to form NH_2• radicals, and eventually produce NH_3. In summary, the active particles generated by plasma under relatively mild conditions exhibit high reactivity, which effectively break the N≡N bond of N_2 molecules and the strong chemical bonds of H_2 molecules, thereby promoting NH_3 generation.

Based on above considerations, it can be concluded that the plasma-catalyzed NH_3 synthesis can circumvent many potential limitations, compared with conventional thermocatalysis. For example, although a high temperature provides energy for N_2 dissociation during the thermocatalysis reaction process, NH_3 only exhibits thermodynamic activity under low temperature. Therefore, it is necessary to simultaneously apply high pressure under high temperature conditions to ensure the reaction rate, thereby shifting the equilibrium reaction to the product. For this reason, Vojvodic et al. [43]. screened the catalysts required for the low-pressure and low-temperature NH_3 synthesis, and defined an ideal scaling relation between the activation energy for N_2 dissociation and the N adsorption energy for characterizing active catalyst, as presented in Figure 3B. Furthermore, the thermocatalysis NH_3 synthesis is limited by the linear relationship between the binding strength of catalyst surface to N-containing species and the N_2 dissociation. On the other hand, the molecular vibration, electron excitation, and electron impact dissociation induced by the high-energy electrons overcome the reaction energy barrier of N_2 activation, during the process of plasma-catalytic NH_3 synthesis. Thus, the translational kinetic energy of molecules, ions and free radicals in the reaction gas remains at a relatively low temperature. At the same time, the N_2 dissociates during the plasma discharge process, prior to the adsorption process of the catalyst, and in consequence the gas-phase substances can be adsorbed on the catalyst surface with a relatively low N_2 binding energy. It is easy to be desorbed from the catalyst surface after the generation of NH_3 without affecting the surface activity. Hence, the plasma-enhanced NH_3 synthesis can not only meet the energy requirements of the reaction at ambient temperature and pressure, allowing it to maintain thermodynamic advantage, but also break the linear relationship between binding strength of N-containing species with catalyst surface and N_2 dissociation [46]. Compared with the adsorption of free N_2 or H_2, the large amount of N and H produced during the plasma discharge greatly changes the thermal balance of NH_3 synthesis and reaction rate. In addition, the electron bombardment and photon radiation caused by plasma discharge also accelerate NH_3 desorption, without observable effect on the catalyst surface. In order to reveal this conclusion, Winter et al. [44]. identified the reaction intermediates adsorbed on the catalysts during the plasma-activated NH_3 synthesis under various temperatures using the Fourier transform infrared (FTIR) spectroscopy, as illustrated in Figure 3C. In the meantime, it is also proved that the NH_3 yield is impacted by the plasma-derived intermediates, together with the interaction between intermediates and catalyst surfaces, resulting in different reaction routes. Rouwenhorst et al. [45]. also confirmed that the plasma-catalytic NH_3 synthesis with excited N_2 can be achieved beyond thermal equilibrium, by experimental data with ruthenium (Ru) catalysts at temperatures above 300°C. The NH_3 yield depends

27662098, 2026, 1, Downloaded from https://onlinelibrary.wiley.com/doi/10.1002/EXP.20240438 by CochraneChina, Wiley Online Library on [08/06/2026]. See the Terms and Conditions (https://onlinelibrary.wiley.com/terms-and-conditions) on Wiley Online Library for rules of use; OA articles are governed by the applicable Creative Commons License

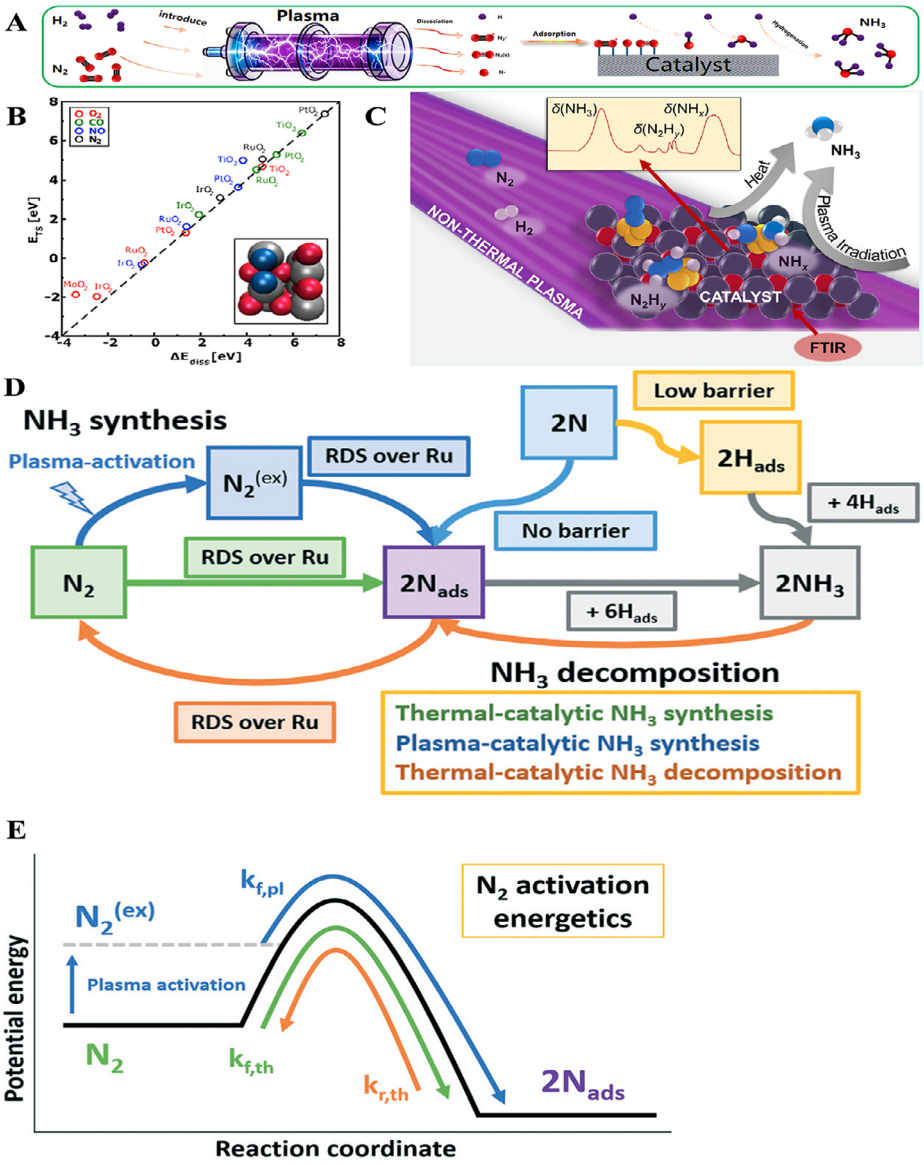


FIGURE 3 | (A) Mechanism diagram of plasma-enhanced NH_3 synthesis. (B) Calculated transition state energies versus dissociative chemisorption energies for N_2, CO, O_2, and NO on the (110) stoichiometric surface of rutile oxides. Reproduced with permission Ref. [43]. (C) Identifying surface reaction intermediates in plasma catalytic NH_3 synthesis via the FTIR spectroscopy. Reproduced with permission Ref. [44]. (D) Schematic representation, and (E) free energy for the thermal-catalytic, plasma-catalytic NH_3 synthesis and thermal-catalytic NH_3 decomposition. Reproduced with permission Ref. [45].

on the competition between dissociative adsorption of basal N_2 and adsorption of plasma-generated N radical species for subsequent hydrogenation to NH_3, along with thermocatalysis decomposition of NH_3 (Figures 3D,E). The plasma-catalytic NH_3 synthesis at temperatures below 300°C is due to the adsorption of N radicals produced in the plasma, and their subsequent hydrogenation to NH_3. These findings suggest that thermally active catalysts are not suitable for use in the plasma catalysis, because these also catalyze the reverse decomposition reactions.

3 | Different Types of Plasma for NH_3 Synthesis

3.1 | Definition

It is well known that matter generally exists in three states, that is, solid, liquid, and gas. Actually, if sufficient energy continues to be added to a gas molecule, it can also be partially or completely converted into plasma state [47]. Plasma is a special state which is different with solid, liquid and gas state. It is considered to be high-energy matter, usually containing free radicals and excited state species [48], which endow it with excellent physical and chemical properties, such as high electrical conductivity, large thermodynamic instability, and very strong coupling effect with electromagnetic field. In addition, plasma possesses high electron temperature, low gas temperature, and high energy density too. Since the concept of "plasma" was first introduced in 1928, it has been used in various fields, and fundamentally changed the development of industrial manufacture and health care [49]. Meanwhile, plasma is also regarded as one of the most promising approaches to activate the N≡N bond, because it can be carried out under ambient conditions with high productivity, thereby effectively boosting the NRR [50]. In this section, a systematic summary for recent reports on the application of

27662098, 2026, 1, Downloaded from https://onlinelibrary.wiley.com/doi/10.1002/EXP.20240438 by CochraneChina, Wiley Online Library on [08/06/2026]. See the Terms and Conditions (https://onlinelibrary.wiley.com/terms-and-conditions) on Wiley Online Library for rules of use; OA articles are governed by the applicable Creative Commons License

TABLE 1 | A comparison of recently reported NH_3 synthesis processes using different plasmas.

Plasma	Catalyst	Feed gas	Power W	NH_3 yield μmol g_{cat}^{-1} min^{-1}	Energy efficiency g-NH_3 kWh^{-1}	Ref.
DBD	0.5Ni/LaOF	N_2:H_2 = 1:3	13	34.94	2.7	[51]
DBD	$La(OH)_3$	N_2:H_2 = 1:3	13	37.13	2.91	[52]
DBD	SBA-15	Air	35	88.95	1.04	[53]
DBD	Ni-MOF-74	N_2:H_2 = 1:1	35.7	85.75	1.27	[54]
DBD	Co-Ni/MOF-74	N_2:H_2 = 1:1	34.57	43.48	0.72	[55]
DBD	Au	N_2:H_2 = 1:1	128.8	/	0.58	[37]
DBD	γ-Al_2O_3	N_2, H_2O	/	0.072	0.0005	[56]
DBD	Ni/LDH-500-P	N_2:H_2 = 1:1	/	75.33	1.71	[57]
DBD	Ru/MgO	N_2, H_2O	/	44.5	0.065	[58]
DBD	Co-N_2	N_2:H_2 = 2:3	59	177.45	0.31	[59]
DBD	La_2O_3	N_2:H_2 = 1:3	13	35.47	/	[60]
DBD	Zeolites	N_2:H_2 = 4:1	6.4	2.3	1.1	[61]
GD	Pt	N_2:H_2 = 5:2	199l5	/	0.12	[62]
MW	/	N_2, H_2	1100	/	0.04	[63]
MW		N_2, Ar, H_2	3000	420.9	/	[64]
MW	Co/γAl_2O_3	N_2, CH_4	180	32.34	0.01	[65]
GAD	/	N_2	/	0.67	0.026	[66]
DC	/	N_2, H_2O	/	5.83	0.0184	[67]

different plasmas in NH_3 synthesis process, along with their advantages and disadvantages is presented in Tables 1 and 2 respectively, in order to gain a deeper understanding of the research and development of plasma-assisted NH_3 synthesis technology.

3.2 | Classification

Plasma can be divided into two main categories, that is, high-temperature plasma and low-temperature plasma. Among them, the latter can be further subdivided into thermal plasma and non-thermal plasma. Different types of plasma exhibit significant differences in the reaction mechanisms and energy efficiency. For the high-temperature plasma, the temperatures of electrons, ions, and background gases are all close to 10^7 K. As for the thermal plasma, the component temperatures are uniform, and approximately 10^4 K. Under the high-temperature conditions of thermal plasma, the N_2 molecules can be dissociated into active species, thereby participating in subsequent reactions. However, most of its input energy is used for gas heating rather than effective chemical reactions, resulting in a higher energy consumption compared with that of current non-thermal plasma or catalyst-assisted system. Furthermore, rapid quenching is required to maintain the stability of NH_3, as high temperatures promote its decomposition. In contrast, the energy is primarily distributed to heat electrons in the non-thermal plasma, enabling electron energies to reach about 10 eV, while the ions and background gases remain at room temperature. At this point, the gas energy is much lower than the electron energy, thereby achieving the efficient dissociation of N≡N bond under ambient conditions. Therefore, the non-thermal plasma with low energy input is expected to significantly reduce the energy loss of conventional N_2 fixation technology [35, 68, 69].

Furthermore, the non-thermal plasma has the characteristics of mild conditions, simple operation, stability, safety, and low cost, so it is widely employed in activation and conversion of N_2 [70]. Since the 1980s, scholars have conducted systematic investigations on the plasma-assisted NH_3 synthesis technology, involving in the reaction devices, raw materials, discharge mode and power, etc. [69]. Some of them try to increase NH_3 yield, or reduce energy consumption by optimizing the technological parameters. In other cases, they are demonstrated that the combination of non-thermal plasma and catalyst provides a unique condition for the transformation of N_2 to NH_3 [51, 71–73]. For instance, the plasma generated by reactant gas under discharge conditions can break through the equilibrium limitations of conventional NH_3 synthesis technology, thereby producing high-density reactants, such as ion, free radical, or vibrationally excited molecule through electron collisions, and initiating a variety of chemical reactions in the gas phase. These studies make non-thermal plasma-assisted NH_3 synthesis an attractive alternative to the Haber–Bosch process. Non-thermal plasma can be generated by the dielectric barrier discharge plasma, glow discharge plasma, microwave discharge plasma, gliding arc discharge plasma, and corona discharge plasma, etc. [51, 71–73]. Different discharge conditions and forms can produce various active species, resulting in significantly distinct activation effects.

27662098, 2026, 1, Downloaded from https://onlinelibrary.wiley.com/doi/10.1002/EXP.20240438 by CochraneChina, Wiley Online Library on [08/06/2026]. See the Terms and Conditions (https://onlinelibrary.wiley.com/terms-and-conditions) on Wiley Online Library for rules of use; OA articles are governed by the applicable Creative Commons License

TABLE 2 | The advantages and disadvantages of different plasma generation methods for NH_3 synthesis.

Plasma	Advantages	Disadvantages
DBD	i. Atmospheric pressure, and simple equipment; ii. Easy to integrate with catalyst; iii. Uniform and stable discharge.	i. By-product generation; ii. High energy consumption; iii. Carbon buildup on electrodes.
GD	i. High yield under low pressure; ii. High concentration of active particles; iii. Controllable reaction pathway.	i. Vacuum environment; ii. Complex and expensive equipment; iii. Difficult to produce continuously.
MW	i. No electrode contamination; ii. High power density; iii. Long life of active particles.	i. High-cost equipment; ii. Complex reactor; iii. Microwave leakage.
GAD	i. High airflow capacity; ii. Significant thermal effect; iii. High energy density and strong ionization.	i. Extremely high energy consumption; ii. Poor stability, and difficult to operate continuously; iii. Severe equipment wear.
CD	i. Simple structure; ii. Quick start; iii. Atmospheric pressure.	i. Limited processing capacity, low efficiency and yield; ii. Weak discharge intensity; iii. Many by-products.

3.2.1 | Dielectric Barrier Discharge Plasma

Dielectric barrier discharge (DBD) plasma requires the insertion of at least one piece of insulating medium in the air gap between two metal electrodes. The insulating medium, mainly consisted of quartz and ceramics, etc., is the key to normal discharge, which can not only limit the charge transfer during the discharge process, thereby making the discharge evenly distributed on the electrode surface, but also avoid the electrode corrosion [74]. At present, there are two modes of dielectric barrier discharge under atmospheric pressure, that is, filamentary discharge and diffuse discharge [75]. In general, the DBD plasma has relatively low ion and gas temperatures, high electron temperature, along with the generation of some high-energy particles, thus it is able to complete discharge reactions at normal temperature and pressure. Moreover, the DBD plasma possesses features of simple device, strong operability, easy integration, and massive production, etc. [76]. Therefore, it has broad application prospects in large-scale gas conversion, and is gradually becoming a research hotspot in the field of plasma-assisted NH_3 synthesis. In recent years, more and more scholars have focused their attention on the conversion of N_2 to NH_3 based on the non-thermal plasma with the DBD technology as the discharge mode [77].

The DBD technology can also be easily coupled with the catalyst, and show an obvious synergistic effect [78–80]. For example, the DBD can offer high-quality energy input to the reaction system, thereby generating highly active vibrationally excited state and active specie (e.g., free radical) by ionizing gas molecules, while the catalyst may provide active sites for the reaction of active species, change the reaction path, and reduce the reaction barrier [81, 82]. In this regard, Feng et al. [56]. synthesized NH_3 from H_2O and N_2 in the DBD plasma reactor filled with Al_2O_3 catalyst under atmospheric pressure and room temperature. The results demonstrate that the catalyst not only offers the adsorption, dissociation, and surface reaction routes towards the NRR reaction, but also significantly enhances the electric field intensity of the reactor, thereby producing more active radicals (e.g., H•, N• and NH_x•) in gas phase, as illustrated in Figure 4A. Therefore, the coupling of DBD plasma and catalyst can boost NH_3 synthesis. To match the DBD plasma reactor, Liu et al. [55]. developed a series of bi-transition metals supported on the traditional catalysts, such as Al_2O_3, MCM-41 and MOF-74, further elevating NH_3 yield and energy utilization. As shown in Figure 4B, the catalytic activity reflected by plasma discharge is in the order of Co-Ni/MOF-74 > Co-Ni/MCM-41 > Co-Ni/Al_2O_3 > Al_2O_3 > plasma only. Among them, the Co-Ni/MOF-74 displayed the maximum yield up to 2608.70 μmol g^{-1} h^{-1} from the reaction gases of N_2 and H_2 with a specific energy input of 33.27 kJ L^{-1} at 200°C. Besides, the DBD plasma-catalytic N_2/H_2O process on the noble metal-based heterostructure, that is, the ruthenium cluster supported on magnesium oxide (Ru/MgO), may also an effective method for NH_3 production under ambient conditions (Figure 4C) [58]. This is because that the high-energy electrons can initiate the plasma catalysis through generating high-density N_2 (v, vapor), while ~87.5% N_2 (v) contributes to the generation of surface-adsorbed N (s, solid). After that, the interaction of NH (s) and H_2 or NH_2 (s), together with atomic H further forms NH_3 (Figure 4D). The catalytic activity of Ru/MgO is significantly superior to other catalysts including MgO, Al_2O_3, and SiO_2, owing to the decreased activation energy towards the dissociative adsorption of N_2 (Figure 4E), while its NH_3 yield is even higher than those of other catalytic procedures, such as electrocatalytic NRR (eNRR), lithium (Li)-intermediary eNRR, and plasma-assisted NRR or eNRR (Figure 4F). Chen et al. [53]. also systematically optimized the synthetic NH_3 ability of DBD plasma-catalytic reaction, through adjusting the system configurations, screening catalyst support materials, and optimizing operating parameters

27662098, 2026, 1, Downloaded from https://onlinelibrary.wiley.com/doi/10.1002/EXP.20240438 by CochraneChina, Wiley Online Library on [08/06/2026]. See the Terms and Conditions (https://onlinelibrary.wiley.com/terms-and-conditions) on Wiley Online Library for rules of use; OA articles are governed by the applicable Creative Commons License

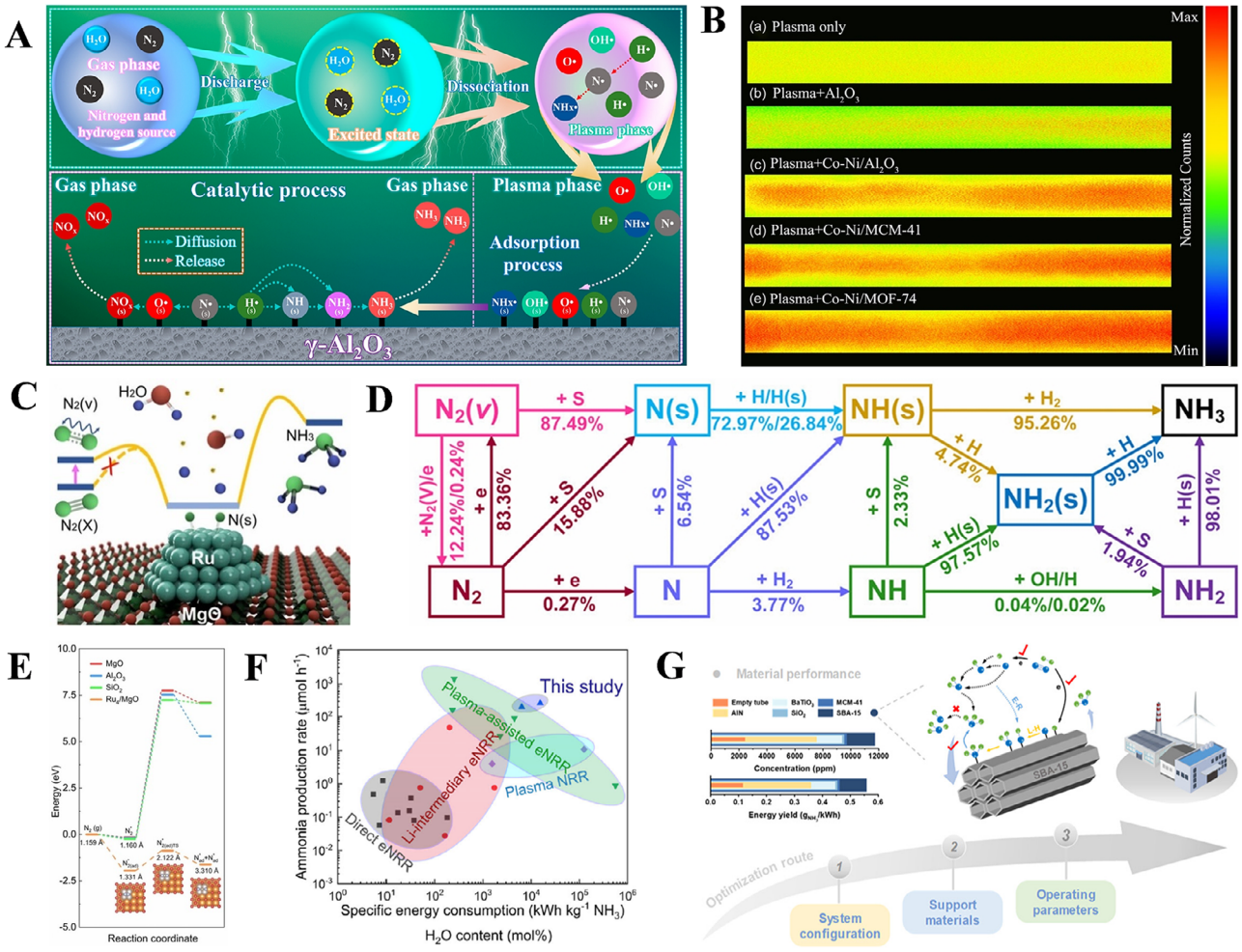


FIGURE 4 | (A) Schematic illustration of reaction routes for NH_3 synthesis by the DBD plasma combined with the γ-Al_2O_3 catalyst. Reproduced with permission Ref. [56]. (B) The intensified charge-coupled device images of plasma discharge in the absence (plasma only) and presence of different catalysts, such as Al_2O_3, Co-Ni/Al_2O_3, Co-Ni/MCM-41 and Co-Ni/MOF-74. Reproduced with permission Ref. [55]. (C) Schematic illustration of decentralized plasma-catalytic synthesis of NH_3 from N_2 and H_2O on the Ru-doped MgO catalyst, (D) possible reaction pathways for the plasma-catalytic NH_3 synthesis of N_2/H_2O system, (E) the N_2 dissociation process over different catalysts, and (F) comparison of NH_3 yield in the direct eNRR, Li-intermediary eNRR, plasma-assisted eNRR, plasma-assisted NRR, and decentralized plasma-catalytic systems. Reproduced with permission Ref. [58]. (G) Schematic diagram for the enhanced mechanism of NH_3 synthesis on the SBA-15 catalyst. Reproduced with permission Ref. [53].

(Figure 4G), thereby achieving a high NH_3 yield of 5337 μmol g_{cat}^{-1} h^{-1} with an energy utilization of 1.04 g_{NH_3} kWh^{-1}.

Unfortunately, limitation still exists, because the energy efficiency of NH_3 synthesis in the DBD plasma is severely limited by the decomposition of NH_3. In this regard, van't Veer et al. [83]. employed a plasma kinetic modeling to gain insight into the formation mechanism of NH_3 in the filled-bed DBD reactor, and proposed that the plasma can both synthesize and decomposed NH_3. Specifically, NH_3 is formed from N• and H• radicals during the afterglow process, and is dissociated by electron collisions during the micro-discharge process, as illustrated in Figures 5A,B. Further experimental evidence for the plasma decomposition of NH_3 is also provided by Navascués et al. [84]. who reveal the deformation behavior of NH_3 in electron collisional plasma, through the isotopic labeling experiment (Figure 5C). In view of the NH_3 decomposition during plasma-chemical fabrication, Peng et al. [85]. introduced a synergistic absorption strategy of magnesium chloride to decrease the influence of product deformation on the energy efficiency of the system, but its stability is poor. To this end, Kevin et al. [61]. used a relatively stable zeolite as the adsorbent for in situ recycling of NH_3 from the DBD system, which effectively suppressed product decomposition. Correspondingly, the yield for plasma-assisted NH_3 synthesis with in situ recovery strategy is 2 times as large as that of steady-state plasma-chemical method (Figure 5D). Besides, Wang et al. [86]. also designed a Ni loaded on ordered mesoporous MCM-41 catalyst (Ni/MCM-41, Figure 5E), for suppressing in situ plasma-induced NH_3 decomposition. Owing to the absence of plasma discharges in the ordered mesopores, the generated NH_3 could diffuse into the mesoporous MCM-41, thus limiting the plasma-induced reverse reaction, resulting in a high yield of more than 60 kJ L^{-1} in the DBD reactor. These encouraging works offer profound insights into the design and synthesis of the catalysts, and point out potential directions for the future development of DBD plasma-enhanced NH_3 synthesis.

27662098, 2026, 1, Downloaded from https://onlinelibrary.wiley.com/doi/10.1002/EXP.20240438 by CochraneChina, Wiley Online Library on [08/06/2026]. See the Terms and Conditions (https://onlinelibrary.wiley.com/terms-and-conditions) on Wiley Online Library for rules of use; OA articles are governed by the applicable Creative Commons License

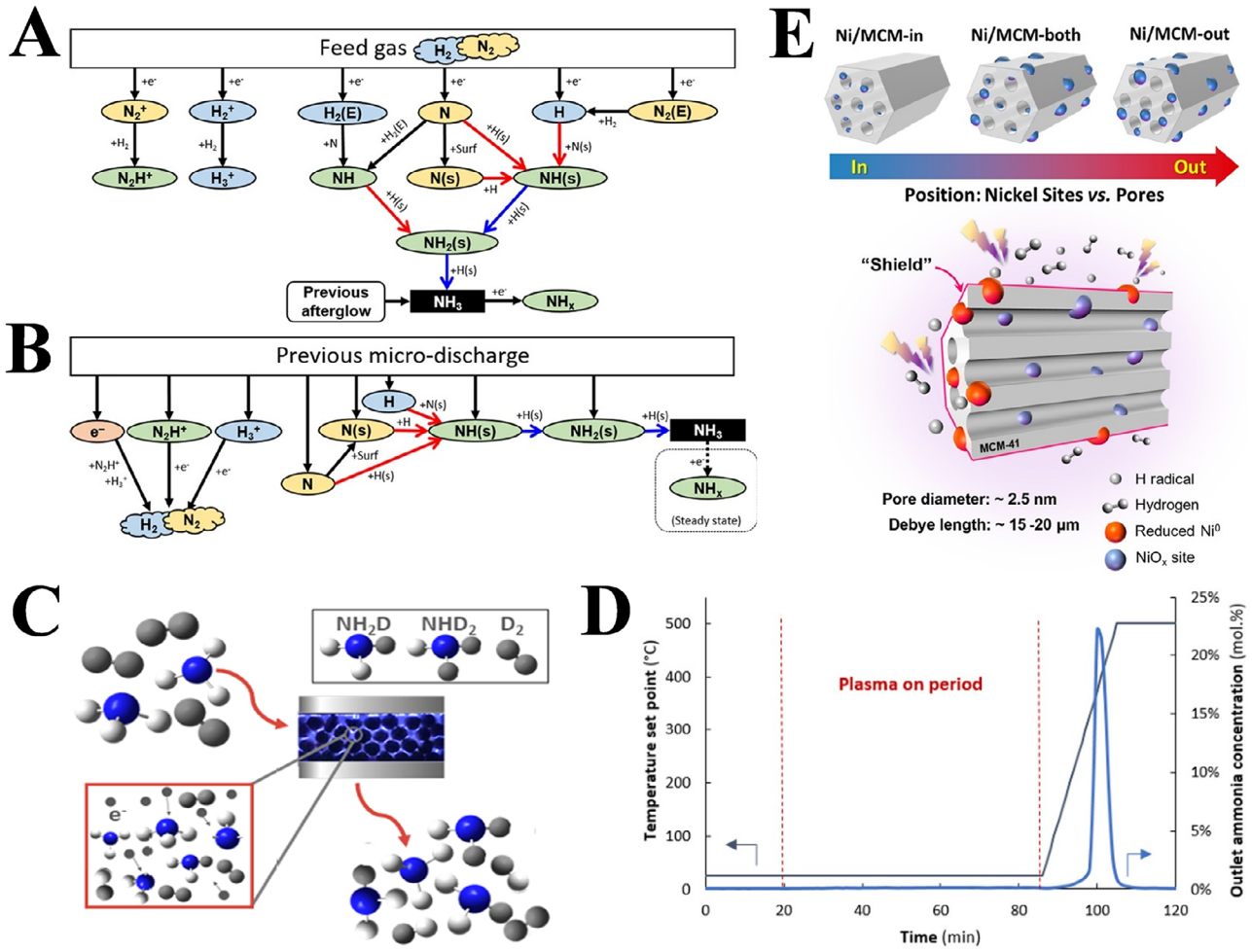


FIGURE 5 | (A) Reaction mechanism of NH_3 generation in the DBD during microdischarge, and (B) its afterglow. Reproduced with permission Ref. [83]. (C) Scheme showing the NH_3 decomposition reaction. Reproduced with permission Ref. [84]. (D) Example experiment for plasma-based NH_3 synthesis with in situ adsorption. Reproduced with permission Ref. [61]. (E) Schematics of the Ni catalysts with mesoporous MCM-41 supports (top), and shielding effect of MCM-41 on Ni within its mesopores in the plasma discharge (bottom). Reproduced with permission Ref. [86].

3.2.2 | Glow Discharge Plasma

Glow discharge (GD) plasma is a low-pressure discharge phenomenon, in which the working pressure is generally lower than 10 mbar. The experimental facility of GD plasma mainly consists of two parallel electrodes placed in a closed container, while its working principle is to use the electrons generated by the GD plasma to excite neutral atoms or molecules, thereby releasing energy in the form of light, as the excited particles fall from excited state to ground state. For example, Bai et al. [87]. employed an ultra-intense narrow-pulse electric field to form a strong GD plasma in a reactor filled with N_2 and H_2. Under the action of GD plasma, N_2 and H_2 can undergo ionization and decomposition reactions at atmospheric pressure, thus producing a large number of free atoms, ions, and free radicals, etc., and forming the non-equilibrium plasma. Subsequently, they were finally synthesized into NH_3 with a concentration of 5000 μL L^{-1} under the control of directional chemical reaction.

In order to reduce energy cost, Pei et al. [88]. systematically investigated the effects of discharge current, gap distance, gas flowrate, tube wall temperature, and catalyst position on N_2 fixation in atmospheric pressure GD plasma (Figure 6A), and achieved a low specific energy of 200–250 GJ tN^{-1}. Previous studies have shown that vibrational excitation could reduce the energy barrier of N_2 fixation reaction, thereby significantly improving the yield of plasma-assisted NH_3 synthesis. Surprisingly little has been reported on the energy efficiency of vibrational-plasma-excited N_2 fixation. Qiao et al. [89]. applied vibrational coherent anti-stokes Raman scattering as a long-pulse air plasma to quantify the time behaviors of rotational and vibrational temperatures of N_2 in the spark and glow modes, for overcoming the challenge of energy efficiency (Figure 6B,C). The results demonstrated that the GD can effectually heat the gas to 3500 K with a vibrational temperature exceeding 5000 K, providing important inspirations for the further investigation of plasma-chemical N_2 fixation derived by vibrational excitation.

Nevertheless, the limit of GD plasma-enhanced NH_3 synthesis still exists compared with other plasma technologies, because it generally occurs under the low pressure and rarefied gas conditions, so its discharge process is unstable. In addition, the glow can easily transition to electric arc, thereby damaging the reactor. All these disadvantages may lead to the decrease in

27662098, 2026, 1, Downloaded from https://onlinelibrary.wiley.com/doi/10.1002/EXP.20240438 by CochraneChina, Wiley Online Library on [08/06/2026]. See the Terms and Conditions (https://onlinelibrary.wiley.com/terms-and-conditions) on Wiley Online Library for rules of use; OA articles are governed by the applicable Creative Commons License

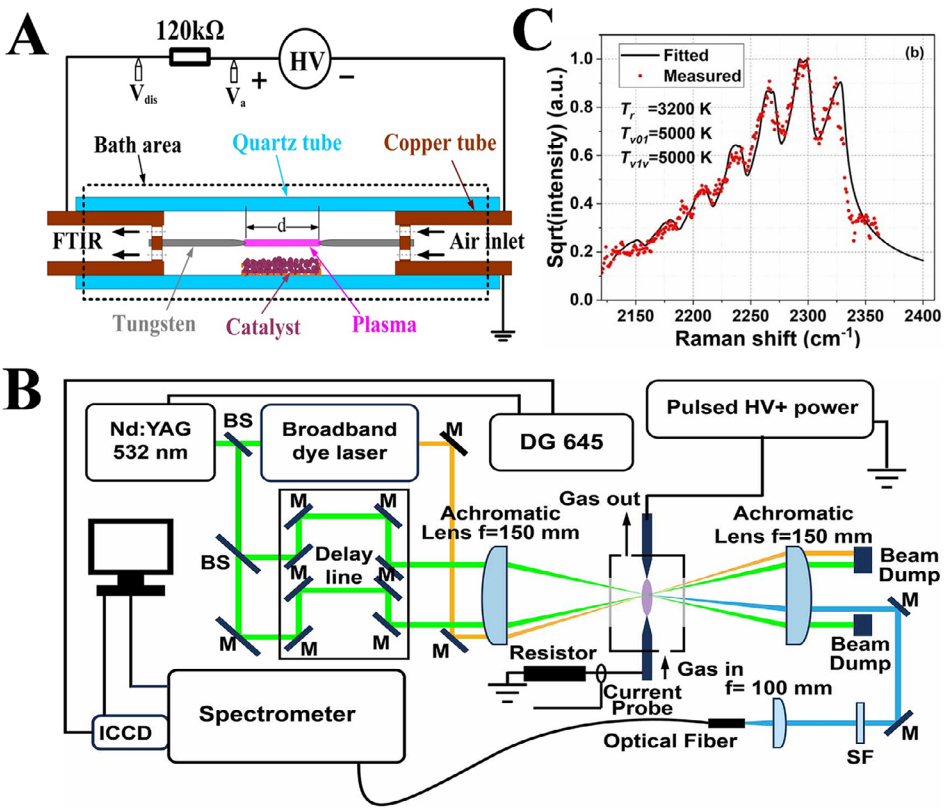


FIGURE 6 | (A) Schematic illustration for the experimental apparatus of NO_x production with the DC-GD. Reproduced with permission Ref. [88]. (B) Schematic drawing for the coherent anti-Stokes Raman scattering (CARS) test of long-pulse air discharge, and (C) corresponding vibrational spectrum of N_2 detected in the GD phase. Reproduced with permission Ref. [89].

NH_3 yield, and therefore little has been reported on the GD plasma-assisted NH_3 synthesis technology.

3.2.3 | Microwave Discharge Plasma

Microwave discharge (MW) plasma is produced from the gas excited by high-frequency electromagnetic field, stemming from the standing wave resonance of microwave in resonant cavity [90]. In general, the microwave frequency is ranging from 0.3 to 10 GHz [91]. In 2008, Nakajima et al. [63]. employed atmospheric pressure microwave plasma to synthesize NH_3, as illustrated in Figure 7A,C. The results demonstrate that the generation of active N-containing groups is a very important factor, during the synthetic process of NH_3. Besides, injecting H_2 into the plasma gas may effectively inhibit the activation of N_2. In contrast, injecting H_2 into the downstream region of the plasma enhances the synthesis of NH_3. Meanwhile, dilution with Ar in the plasma gas can also significantly promote the formation of N-containing active groups. Hu et al. [64]. developed a MW plasma-enhanced reactor (Figure 7B) to pre-activate N_2 before the catalytic reaction, thereby achieving the chemical cycle of NH_3 with a high yield of 420.9 μmol min^{-1} g^{-1} under mild nitriding condition and atmospheric pressure. Figure 7D depicts the possible reaction mechanism. As shown, the MW plasma is initiated, when the catalyst bed reaches the temperature of nitridation ($T_{nitridation}$, Figure 7D–1). The N_2 is introduced into the system after the plasma is stable, followed by the nitridation reaction (Figure 7D–2). Subsequently, the activated N-species accumulate and react with the catalyst surface (Figure 7D–3), and a nitride diffusion layer is appearance (Figure 7D–4). Once the activation processing is complete, the plasma is stopped, while the rest of N_2 is discharged from the system with Ar flow (Figure 7D–5). Then, the system temperature is regulated to a level suitable for the hydrogenation reaction, accompanied by the introduction of H_2 (Figure 7D–6). At the moment, NH_3 is released from the activated species-adsorbed surface, because of the ease of H_2 dissociation and diffusion in bulk Fe (Figure 7D–7). At last, the NH_3 yield gradually reduces and eventually stops, as most of the lattice N_2 is removed (Figure 7D–8). This novel strategy based on the Fe catalyst exhibits more obviously advantages in the yield of activated species, modularity, fast startup, and low voltage input, compared with similar plasma-catalytic technologies. The MW plasma presently still faces the challenges such as high cost and complex structure, compared to other types of plasma. Additionally, the localized micro-discharges or Joule heating effects can easily lead to catalyst sintering. Future efforts should focus on optimizing reactor design, developing suitable catalyst, and further improving energy efficiency to promote the application of MW plasma in enhanced NH_3 synthesis.

3.2.4 | Gliding Arc Discharge Plasma

The gliding arc discharge (GAD) plasma is derived from the fact that the gas is broken down under the excitation of strong electric field, thereby forming the arc at the shortest point of discharge electrode gap. Then, the arc slides along the electrode to generate

27662098, 2026, 1, Downloaded from https://onlinelibrary.wiley.com/doi/10.1002/EXP.20240438 by CochraneChina, Wiley Online Library on [08/06/2026]. See the Terms and Conditions (https://onlinelibrary.wiley.com/terms-and-conditions) on Wiley Online Library for rules of use; OA articles are governed by the applicable Creative Commons License

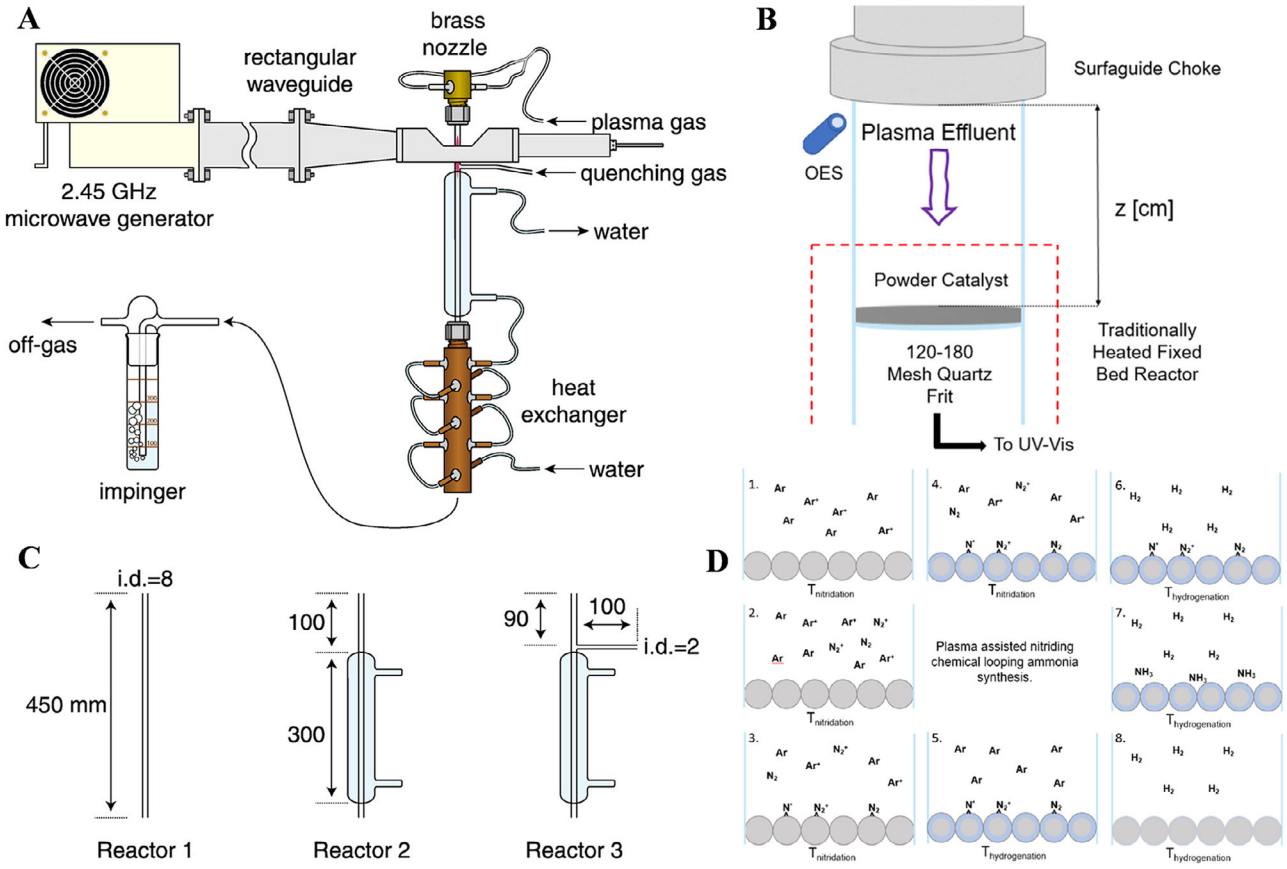


FIGURE 7 | (A) Schematic illustration for the experimental apparatus, and (C) reactors of MW plasma. Reproduced with permission Ref. [63]. (B) Reactor-catalyst-plasma generating system, and (D) plasma-surface mechanism. Reproduced with permission Ref. [64].

a gliding arc under the action of gas flow, and periodically carries out the cyclic process of breakdown-elongation-arc quenching-breakdown [92, 93]. The GAD plasma owns various features, including simple electrode structure, and easy to control, etc. In the meantime, it is also a low-temperature plasma, which can achieve high energy density and large processing capacity and thus, the oxynitride (NO_x) synthesized by the GAD plasma may obtain a higher yield than the individual plasma [94, 95]. Within a certain range of approximate field strength, up to more than 90% of electron energy in the GAD is utilized in the form of vibrational excitation. This allows most of the input energy to be used for the N_2 activation, which is conducive to improving the reaction efficiency, and reducing energy loss. For this purpose, Indumaty et al. [66]. studied the synthesis of NH_3 in a GAD reactor containing the N_2 plasma and aqueous media without the catalyst, as shown in Figure 8A. During the GAD process, a plasma plume was formed, and it could be observed vibrational and rotational excitations on the top of plasma plume in contact with water below (Figure 8B), thereby boosting the NH_3 formation. The NH_3 concentration was 2.12–5.69 ppm, while its production rate varied in the range of 0.63–0.68 mg h^{-1}, depending on the plasma exposure time. This is confirmed by an increase in the vibrational temperature from 2632 K (Figure 8C, D-1 zone) to 3778 K (Figure 8C, D-4 zone), meaning more enhanced electron energy distribution of vibrational excitation (~24%), compared with the electronic excitation (~0.03%). The maximum productivity of this GAD reactor is 0.68 mg h^{-1} with an energy efficiency of 26.8 mg kWh^{-1}. This work therefore demonstrates that the GAD plasma can produce green NH_3 in the absence of catalyst. The GAD plasma requires a strong electric field to form and maintain an arc for now, which slides along the electrode surface. This leads to the issues, for example, high energy consumption, easy damage to the catalyst surface, difficulty in continuous operation, and severe wear of equipment. Therefore, it is usually not suitable for NH_3 synthesis using N_2, H_2 or H_2O as raw materials.

3.2.5 | Corona Discharge Plasma

Corona discharge (CD) plasma is a locally self-sustained discharge phenomenon, occurring in the uneven electric field formed by the gas medium at asymmetric electrodes under atmospheric or high-pressure conditions. When a voltage slightly lower than the breakdown voltage is added to two discharge electrodes, while the local field strength near the electrode surfaces also exceeds the ionizing field strength of the gas, the gas medium near the electrodes is ionized or dissociated by the localized breakdown. At the same time, the gas insulation is destroyed, and the internal resistance decreases, together with a dim glow appearance around the electrode, that is the CD phenomenon [97, 98]. In this respect, Luo et al. [96]. reported a plasma electrolysis system, in which the plasma was generated by an air-pulsed positive direct current CD (Figure 8D), and selectively synthesized either HNO_3 or NH_3 over the Cu_2O nanowire electrocatalyst (Figure 8E,F) from the air through an electrolyte

27662098, 2026, 1, Downloaded from https://onlinelibrary.wiley.com/doi/10.1002/EXP.20240438 by CochraneChina, Wiley Online Library on [08/06/2026]. See the Terms and Conditions (https://onlinelibrary.wiley.com/terms-and-conditions) on Wiley Online Library for rules of use; OA articles are governed by the applicable Creative Commons License

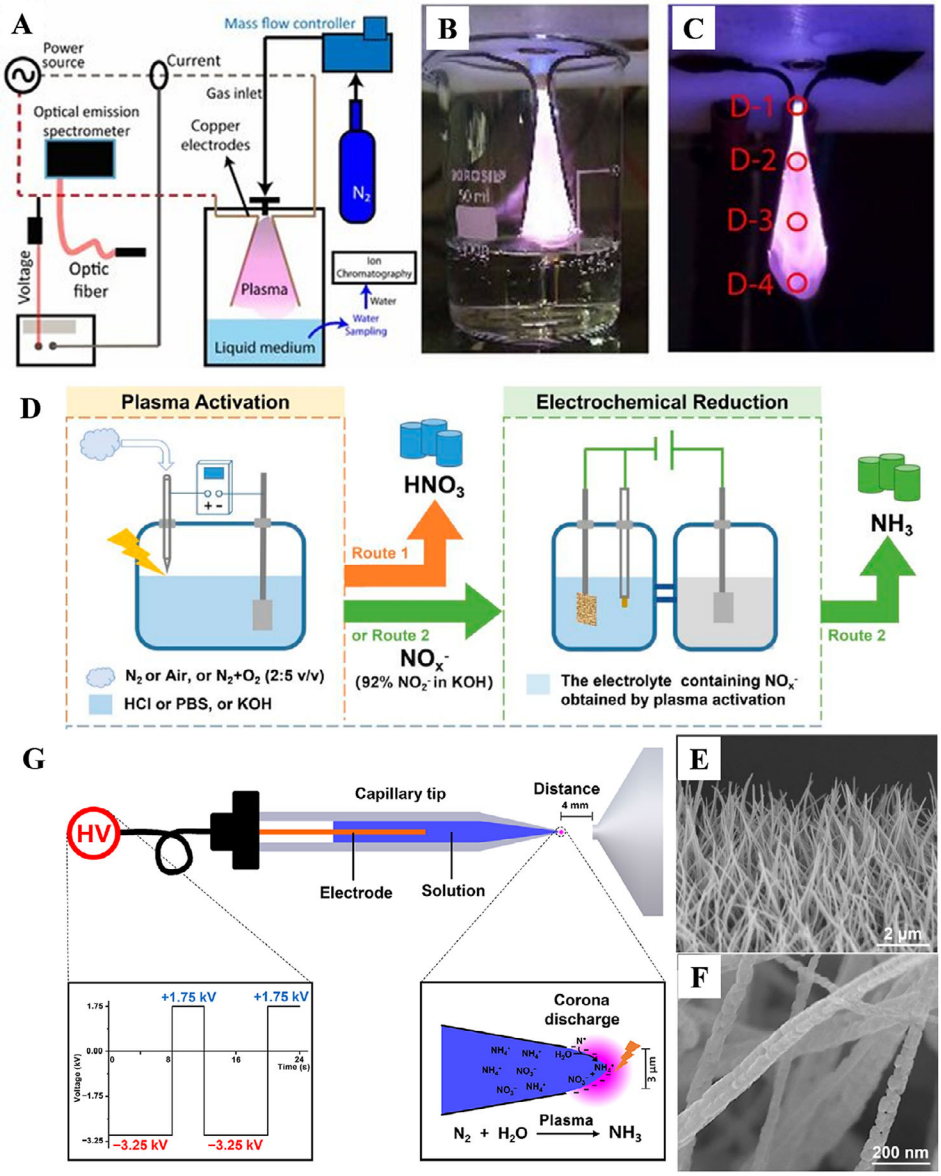


FIGURE 8 | (A) Schematic illustration for the experimental setup of NH_3 synthesis based on the GAD plasma with N_2 as the inlet gas, (B) photograph of the GAD plasma inside the beaker interacting with H_2O surface, and (C) snapshot of the arc captured at an exposure of 0.6 s. Reproduced with permission Ref. [66]. (D) Illustration of the integrated CD plasma and electrochemical system, and (E, F) SEM images of Cu_2O/Cu catalyst. Reproduced with permission Ref. [96]. (G) Schematic setup of the system for NH_3 synthesis using the PR-nESI device. Reproduced with permission Ref. [67].

conditioning strategy. The lowest total energy consumption for the synthesis of NH_3 is 3.91 kWh mol^{-1}. Fang et al. [67]. also proposed the in-situ synthesis and measurement of NH_3 from N_2 by the nanoelectrospray-based CD plasma coupled with the mass spectrometry. The reaction and analysis are achieved via a polarity reversal nanoelectrospray ionization (PR-nESI) device, as presented in Figure 8G. For instance, the plasma is generated by the CD at the capillary tip during the negative polarity half-week, and then N_2 is immobilized through the interfacial reactions and converted to NH_3 in liquid H_2O. It is found that the distance between plasma and H_2O surface plays a decisive role in N_2 immobilization, due to the short lifetime of active plasma. This study was carried out in the presence of plasma with both inverted polarity and plasma, in which the plasma was generated on the surface of a Taylor cone, and the plasma was in direct contact with the H_2O surface. The whole process ensured effective N_2 fixation and NH_3 synthesis. The CD plasma has become an effective tool for exploring the mechanisms of plasma-catalytic NH_3 synthesis, because of its simple setup structure and inexpensiveness. However, its shortcomings, such as weak discharge intensity, low energy efficiency, poor stability, and by-product generation, result in a weaker competitiveness compared with those of other plasma technologies.

4 | Synergistic Effect of Plasma and Catalysis

4.1 | Plasma Coupled With Electrocatalysis

Recently, the plasma-integrated electrocatalysis is recognized as an alternative system to the traditional electrocatalytic process towards the NH_3 synthesis from N_2 and H_2O. In this system, the

27662098, 2026, 1, Downloaded from https://onlinelibrary.wiley.com/doi/10.1002/EXP.20240438 by CochraneChina, Wiley Online Library on [08/06/2026]. See the Terms and Conditions (https://onlinelibrary.wiley.com/terms-and-conditions) on Wiley Online Library for rules of use; OA articles are governed by the applicable Creative Commons License

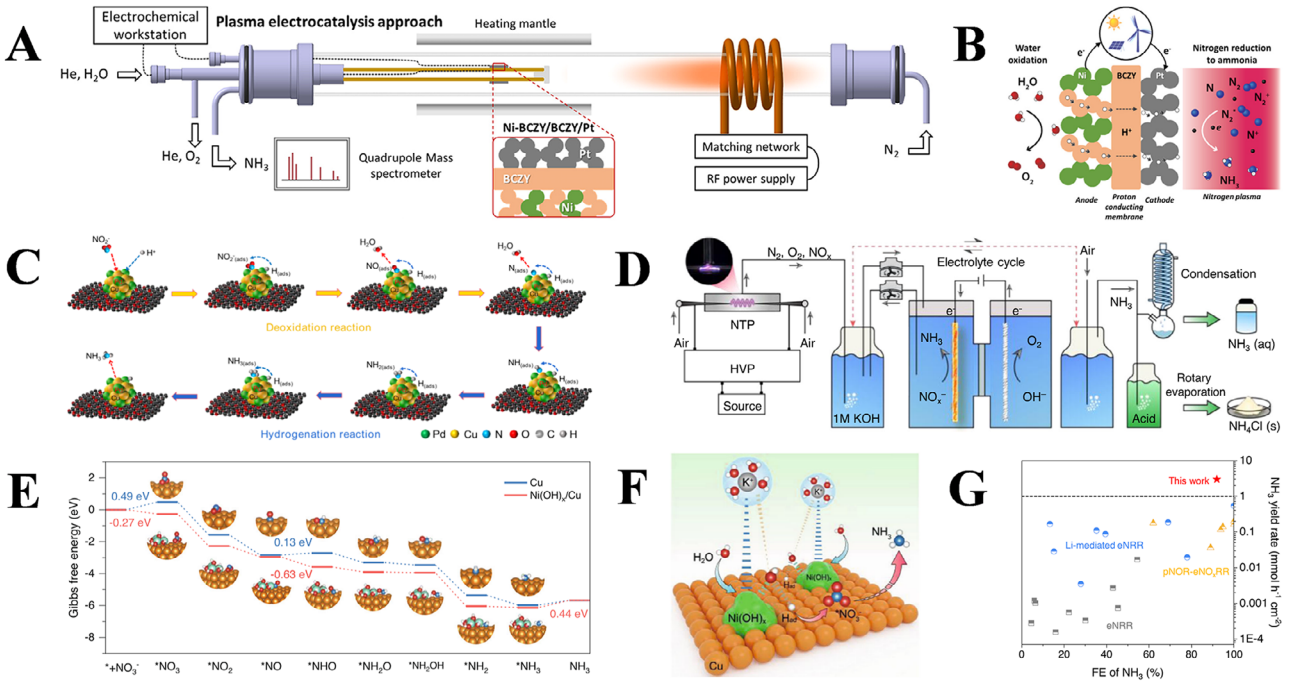


FIGURE 9 | (A) Schematic representation of hybrid plasma electrochemical reactor, and (B) NH_3 production from N_2 and H_2O using a plasma-activated proton conducting solid oxide electrolyzer. Reproduced with permission Ref. [99]. (C) Schematic illustration of the eNO_2^-RR mechanism on the Cu_2Pd/CBC catalyst. Reproduced with permission Ref. [100]. (D) Schematic of pNOR-eNO_x^-RR system and NH_3 products collection, (E) Gibbs free energy diagram of eNO_3^-RR on the Cu and $Ni(OH)_x/Cu$ catalysts, (F) schematic illustration for the role of $Ni(OH)_x$ species in promoting H_2O activation and N-containing intermediates hydrogenation on Cu, and (G) comparison of the NH_3 yield and FE with previous reports, including the eNRR, Li-mediated eNRR, and pNOR-eNO_x^-RR. Reproduced with permission Ref. [101].

plasma is used for activating N_2, thereby reducing the energy barrier of subsequent electrocatalytic NRR. For this purpose, Sharma et al. [99]. established a plasma-assisted electrochemical device (Figure 9A), in which the H_2 produced from the oxidation reaction of H_2O on anode is transported to cathode via a proton conducting membrane (Figure 9B), and subsequently reacts with the plasma-activated N_2 to form NH_3 with yield and Faradaic efficiency (FE) of up to 26.8 nmol s^{-1} cm^{-2} and 88%, respectively. Li et al. [100]. also proposed an integrated strategy combining low-temperature plasma technology with electrochemical reduction, in which the plasma firstly drove the air activation to form nitrite ion (NO_2^-), followed by an electrochemical NO_2^- reduction reaction (NO_2^-RR) to produce NH_3 with a yield of 1956.65 μg h^{-1} mg^{-1}. The possible NO_2^-RR route is also proposed, wherein the reaction involves in three steps of deoxidation and hydrogenation reactions, as illustrated in Figure 9C. Similarly, Liu et al. [101]. also proposed a tandem system of plasma-driven N_2 oxidation reaction coupled with electrochemical NO_x reduction reaction (pNOR-eNO_x^-RR, Figure 9D), and revealed that the adsorption and hydrogenation processes of reactive nitrogen species (NO_x^-) occurred more easily on the $Ni(OH)_x/Cu$ than on the Cu surface (Figure 9E). It is because the $Ni(OH)_x$ on Cu enriches hydrated cations (K^+) in the double layer, owing to the noncovalent interactions. And the H_2O near the catalyst surface can be facilely adsorbed and dissociated on their interfaces, thereby producing H_{ad} to take part in the subsequent hydrogenation reactions of N-containing intermediates adsorbed on the Cu towards NH_3 (Figure 9F). Therefore, the pNOR-eNO_x^-RR system based on the $Ni(OH)_x/Cu$ catalyst may achieve a high NH_3 yield of 3 mmol h^{-1} cm^{-2} along with a FE of 92%, which outperforms those of previously reported Li-mediated eNRR and eNRR processes (Figure 9G).

Moreover, Meng et al. [102]. synthesized the nitrates/nitrites (NO_x^-), through introducing a titanium (Ti) bubbler into the air plasma activation system, and directly used the obtained NO_x^- aqueous solution as a cathodic electrolyte for the following electrocatalytic NO_x^-RR over the cobalt oxide (Co_3O_4) nanoparticles enriched with oxygen vacancies. This novel plasma-electrocatalytic system exhibited remarkable NH_3 yield of 39.60 mg h^{-1} cm^{-2} and corresponding high FE of 96.08%. Liu et al. [103]. also developed a pNOR-eNO_x^-RR system based on the highly dispersed copper-iron (Cu-Fe) nanoalloy for directly synthesizing NH_3 from air, which exhibited high NH_3 yield (190.46 μmol h^{-1} cm^{-2}) and FE (93.74%).

In general, the high energy consumption of plasma-assisted catalysis is considered to be the keypoint where the improvement is the most needed. Now, it has been well demonstrated that the energy efficiency of N_2 activation could be significantly improved by combining plasma with electrochemical process, thereby reducing the energy barrier for subsequent NRR. This is mainly due to the fact that the plasma-electrocatalytic integrated strategy can achieve the leap in energy efficiency of NH_3 synthesis, through the efficient utilization of vibrationally excited N_2. At the same time, the new interfacial reaction mechanism also releases its application potential. In addition, its distributed system powered by renewable energy can further reduce the cost of green NH_3, approaching the critical point of the coal-based H-B process. Hence, the hybrid system coupling plasma

27662098, 2026, 1, Downloaded from https://onlinelibrary.wiley.com/doi/10.1002/EXP.20240438 by CochraneChina, Wiley Online Library on [08/06/2026]. See the Terms and Conditions (https://onlinelibrary.wiley.com/terms-and-conditions) on Wiley Online Library for rules of use; OA articles are governed by the applicable Creative Commons License

and electrochemical process may offer an opportunity to reduce energy consumption, and achieve satisfactory results in terms of NH_3 yield and FE [104]. Although the plasma coupled with electrocatalytic technology shows the potential to break through traditional energy barriers, its large-scale application still faces many practical challenges and path dependencies. For instance, the non-uniform transfer of plasma-generated active nitrogen species at the gas–liquid–solid phase interface results in insufficient utilization of reaction sites on the electrode surface, which remains the primary bottleneck of interfacial mass and energy transfer in the plasma-electrocatalytic system. The high price of noble metal catalysts may restrict its industrial applications, as well. Furthermore, energy matching and process intensification are issues that need to be considered in the distributed NH_3 production industry. It is believed that the industrialization process of plasma-electrocatalytic NH_3 synthesis will eventually become a reality, with the maturity of technologies, such as the optimization algorithm of pulse discharge time and sequence, anti-plasma corrosion electrode as well as coating, etc.

4.2 | Plasma Coupled With Photocatalysis

In 2016, Haruyama et al. [105]. proposed a new NH_3 synthesis approach. The biggest difference from the above methods is that the reaction occurs at the surface of plasma gas phase and H_2O liquid phase under the irradiation of ultraviolet (UV) light. The H_2 source is from H_2O during the reaction to synthesize NH_3. Besides, the authors innovatively introduced the photochemical reactions into the plasma-enhanced NH_3 synthesis process under ambient temperature and pressure without any catalyst (Figure 10A). For instance, the ionized plasma N_2 (gas phase) is passed into a reactor containing H_2O (liquid phase), and then the plasma-liquid (P/L) interface is irradiated with the UV light at wavelengths of 185 nm and 254 nm to synthesize NH_3. During this P/L reaction, the synthetic pathway may mainly involve in the following three steps: (i) the N_2 in the plasma atmosphere first generates a large number of activated state atomic nitrogen (N) through the inelastic collisions; (ii) subsequently, the plasma-activated N is in contact with the liquid-phase H_2O to form NH• under the UV irradiation, followed by NH_2• formation at the P/L interface; (iii) finally, the NH_2• further reacts with H_2O to produce NH_3. Lamichhane et al. [106]. further combined photo-electrochemical H_2O splitting with plasma system, wherein the N generated by the plasma may react electrochemically with hydrogen ions (H^+) obtained from the UV-induced H_2O decomposition, thereby producing NH_3 on the P/L interface, as depicted in Figure 10B. This synergistic strategy can be operated under ambient temperature and pressure using the N_2 and H_2O as the raw materials without any catalyst or sacrificial reagent, while the NH_3 yield is about six times as large as that of individual plasma. Furthermore, Peng et al. [107]. used the spray-type jet plasma and UV light to synergistically excite vapor and liquid H_2O molecules for boosting N_2 fixation, which significantly raised the yields of nitrite (NO_2^-), nitrate (NO_3^-) and NH_3 with the highest values of 15.1, 40.3 as well as 2.5 mmol min^{-1}, respectively. The co-synthesis of NO_2^-, NO_3^- and NH_3 is probably ascribed to the gas phase reaction, liquid phase reaction, as well as their interaction. Specifically, in the gas phase reaction, the electron excites N_2 and vaporized H_2O to produce nitrogen free radicals and hydroxyl radicals, respectively (Figure 10C). While in the liquid phase reaction, the N_2 along with its related free radicals reacted with H_2O to further generate NH_3 under the irradiation of UV light (Figure 10D).

In addition to the N, there are many reactive nitrogen species existing in the plasma, such as excited state N_2* and nitrogen molecular ions (N_2^+) classified according to excitation energy level, and they have different lifetimes and reactivity. Sakakura et al. [108]. quantified the discharge-excited N, N_2* as well as N_2^+, and demonstrated experimentally the effect of reactive nitrogen species with different lifetime, stability and property, along with their plasma-enhanced photo-catalytic reaction mechanism, separately. Figure 10E–G schematically illustrated the experimental conditions of vacuum ultraviolet/ultraviolet (VUV/UV) radiated P/L interfacial reaction. Among them, the plasma is obtained from the DBD (Figure 10E), and the stability of N is measured through changing the distance between discharge locus and photo-detector (Figure 10F), while the relationship between NH_3 yield and P/L reactor is also investigated by varying the distance between discharge locus and H_2O surface (Figure 10G). When the VUV/UV radiation was employed during the reaction between plasma gas phase and aqueous phase, the UV irradiation could promote the N-compounds formation from N_2* and N_2^+ instead of N. These results suggest that the P/L interfacial reactions starting from N or N_2* and N_2^+ follow different reaction mechanisms, and the UV-irradiated aqueous phase may generate H• and •OH, thereby hastening NH_3 synthesis.

4.3 | Plasma Coupled With Thermocatalysis

Although the N_2 activation process under mild conditions favors the thermodynamics of NH_3 synthesis, a proper temperature also plays a key role in accelerating its kinetics. In this respect, Jensen et al. [109]. elevated the efficiency of plasma-assisted NH_3 synthesis by 20% through raising the operating temperature from 100°C to 200°C, proving that appropriate temperature increase could significantly promote the synthesis rate of NH_3. Wu et al. [110]. also presented a novel NH_3 synthesis system combined laser-induced plasma and laser-generated local temperature field, which was significantly superior to that of conventional thermocatalysis. Figure 11A schematically illustrates this laser-induced ammonia synthesis (LIAS) device, in which a high-temperature center is generated at the focal point of target under the laser irradiation, as shown in Figure 11B. The surrounding gas can be collided and ionized into plasma via the free electrons excited by the target, and meanwhile the laser irradiation creates a localized temperature field and a gradient temperature field through thermal diffusion, which meet the requirements of N_2 activation and NH_3 synthesis at different temperatures. And the NH_3 yield of LIAS process can be increased with the acreage of central region (Figure 11C). The LIAS achieves an initial NH_3 yield of 70.8 μmol g^{-1} min^{-1} accompanied by a high H_2 conversion of 9.5% with Fe as catalyst, and a stable yield of 23.63 μmol g^{-1} min^{-1} with a H_2 converting ratio of 3.2% using iron nitride (Fe_4N), because the energy barrier of rate-limiting step on Fe is smaller than that on Fe_4N (Figure 11D). As for their reaction mechanism, the N_2 is ionized into N plasma in the central region by laser radiation over Fe, while the N plasma is migrated to the annular region for NH_3 synthesis under the catalytic effect of Fe and Fe_4N (Figure 11E).

27662098, 2026, 1, Downloaded from https://onlinelibrary.wiley.com/doi/10.1002/EXP.20240438 by CochraneChina, Wiley Online Library on [08/06/2026]. See the Terms and Conditions (https://onlinelibrary.wiley.com/terms-and-conditions) on Wiley Online Library for rules of use; OA articles are governed by the applicable Creative Commons License

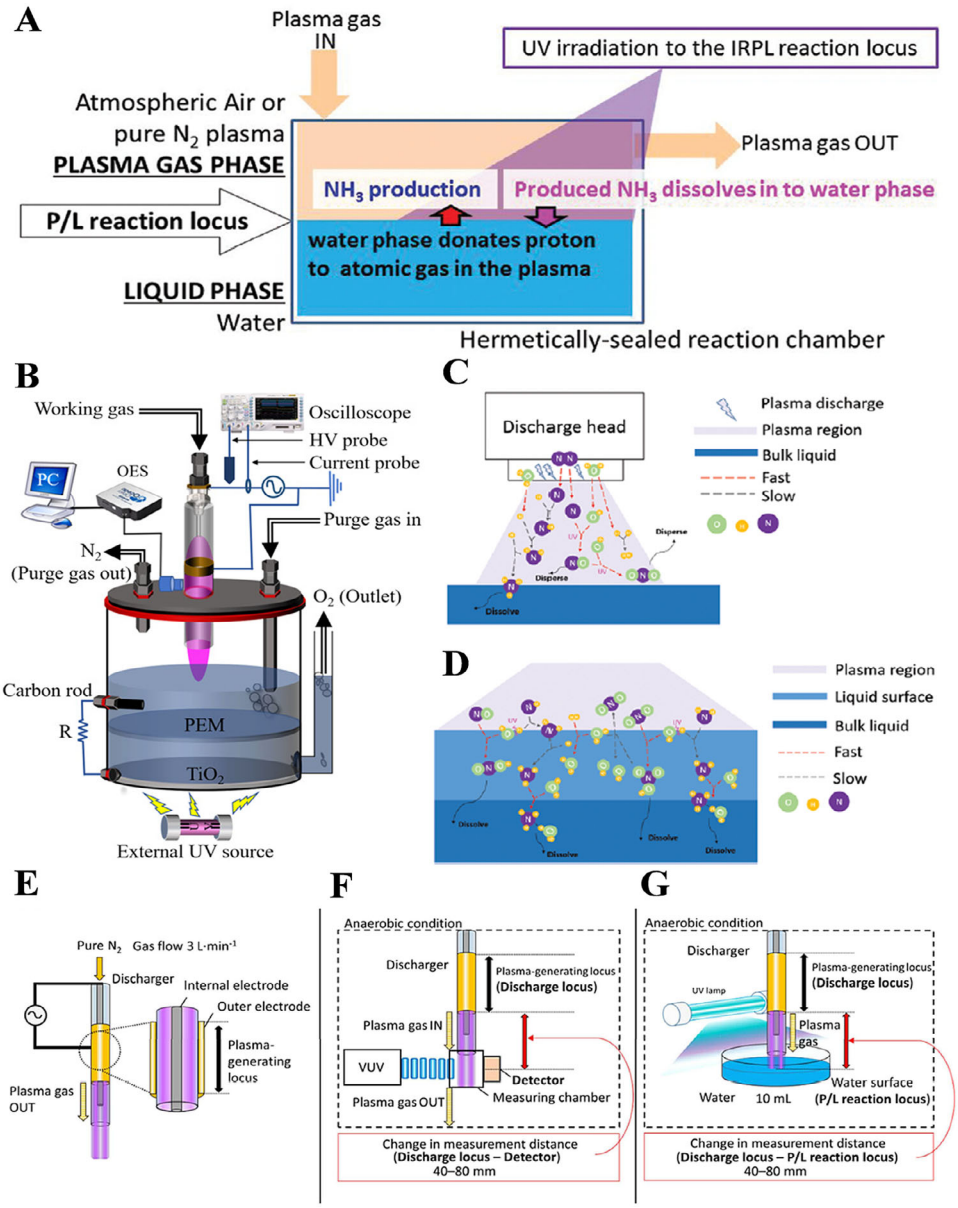


FIGURE 10 | (A) Construction of the interfacial reactor between plasma phase and liquid phase (P/L) for NH_3 synthesis. Reproduced with permission Ref. [105]. (B) Schematic diagram of N_2 plasma jet impinging on the electrolyte at the cathode side of photo-electrochemical H_2O splitting reaction cell together with a proton exchange membrane (PEM). Reproduced with permission Ref. [106]. (C) Mechanism for the in situ jet plasma N_2 fixation in the gas phase, and (D) at the liquid surface. Reproduced with permission Ref. [107]. (E) Illustration of dielectric barrier discharge device for the excited N_2 gas production, and (F) pure N_2 is introduced into the discharger to produce N-plasma, which is introduced into the measuring chamber, or (G) H_2O in a flat glass dish. Reproduced with permission Ref. [108].

Recently, Hu et al. [111]. designed an environmentally friendly plasma thermocatalysis process composed by the DBD reactor and the M/CeO_2 or M/MgO (M = Ru, Fe) catalyst, for sustainable synthesis of NH_3 at atmospheric pressure. The highest NH_3 yield of 6.8 mmol g^{-1} h^{-1} is achieved at 400°C on the Ru/CeO_2, which is far superior to those reported in the literatures using the DBD reactor alone. In addition to the plasma-mediated gas-phase and catalytic surface reactions, the increase in NH_3 concentration under the plasma-catalyzed conditions may be attributed to the synergistic effect between plasma and catalyst, wherein the plasma promotes the desorption of NH_3 and NH_x. Muzammil et al. [112]. also developed a hybrid system combined plasma-generated NO_x with thermocatalysis process, which delivered higher NH_3 selectivity (95%) and yield (7348 mg h^{-1}) than those of other plasma-catalytic approaches. Table 3 summarizes the development status of electrocatalysis, photocatalysis, and thermocatalysis coupled with plasma system for NH_3 synthesis in detail. These studies demonstrate that the performance of NH_3 synthesis can be effectively enhanced through the precise control of temperature field, synergistic effect of plasma and thermal catalysis, and innovative reaction pathway. In the meantime, they also offer insights into the design of efficient reactors and matching catalysts that integrate the temperature control, plasma activation, and optimization of catalytic reaction, thereby pointing the way to future development of efficient and sustainable NH_3 synthesis technologies.

27662098, 2026, 1, Downloaded from https://onlinelibrary.wiley.com/doi/10.1002/EXP.20240438 by CochraneChina, Wiley Online Library on [08/06/2026]. See the Terms and Conditions (https://onlinelibrary.wiley.com/terms-and-conditions) on Wiley Online Library for rules of use; OA articles are governed by the applicable Creative Commons License

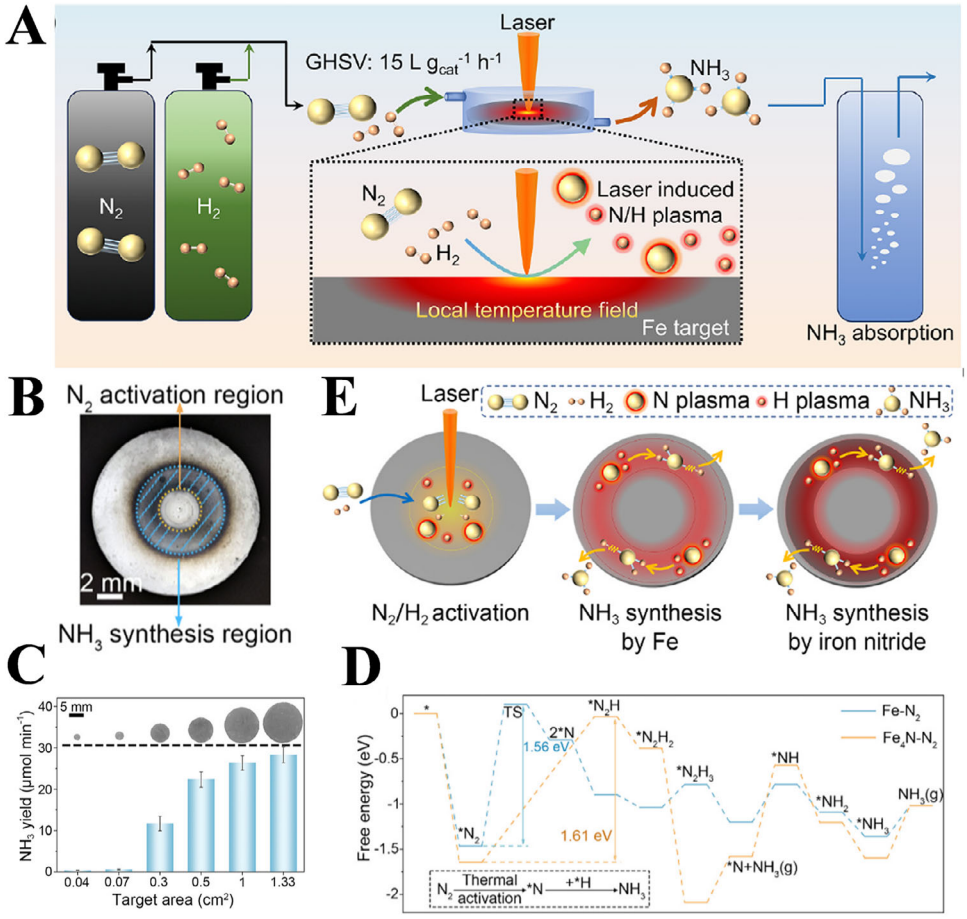


FIGURE 11 | (A) Schematic exhibition of the LIAS process, (B) the optical image of different functional regions on the Fe target, (C) the NH_3 yield with different Fe acreage, (D) the energy profiles of NH_3 synthesis process based on the DFT calculations, and (E) schematic diagram of catalytic mechanism of the LIAS process. Reproduced with permission Ref. [110].

4.4 | Synergistic Effect Between Plasma and Catalyst

The synergistic effect between plasma-activated N_2 and catalyst surface plays a crucial role in the efficiency improvement of NH_3 synthesis. This synergistic mechanism significantly reduces the high activation energy barrier of traditional thermal catalytic processes, thereby providing the core driving force to achieve efficient NH_3 synthesis at ambient conditions. Ma et al. [131]. used a porous platinum (Pt) film deposited on the yttria-stabilized zirconia tubes as a catalyst in this respect. The results demonstrate that the high-density step sites and barrier-free adsorption channels offered by the porous Pt membrane and its surface respectively make the N radicals generated by the RF discharge plasma easier to dissociate and adsorb. At this time, the energy barrier of N_2 dissociation at the step sites becomes the core site for plasma activation of N_2, as illustrated in Figure 12A. As a result, the plasma activates N_2 to produce highly active species, and the catalyst exposes defect sites to lower the reaction energy barrier. In addition, the efficient N_2 fixation can be achieved at room temperature, by optimizing the nanostructure of the catalyst to further increase the interaction interface. Luo et al. [132]. also developed a Ni-Co/CeO_x catalyst with atomic-level dispersion of Ni and Co on the surface of CeO_2 through the hydrothermal method. Among them, the Ni single atoms may reduce the formation energy of oxygen vacancies, causing the enrichment of oxygen vacancies (Figure 12B), while the Co single atoms can strengthen the adsorption of ·H. At the same time, the oxygen vacancies also provide an unsaturated coordination environment to reduce the ·H adsorption energy. The catalyst utilizes oxygen vacancy-single atom dual active sites to synergistically regulate the highly active free radicals provided by the plasma, ultimately achieving a NH_3 yield of 94.3 μmol g^{-1} h^{-1} with a high selectivity of ~100%. Furthermore, it is demonstrated that the free radicals synthesize NH_3 through the E-R mechanism rather than the traditional L-H mechanism. In the existing pNOR-eNO_x^-RR system, the H_2O dissociation rate of Cu catalyst is relatively slow in alkaline environment, resulting in insufficient supply of adsorbed H_2. For this reason, Liu et al. [101]. proposed a unique Ni$(OH)_x$/Cu catalyst, through depositing amorphous Ni$(OH)_x$ on the Cu surface. The Ni$(OH)_x$/Cu interface may attract hydrated cations in the electrolyte via the non-covalent interactions, thereby forming a local high-concentration cation environment. The enriched cations further weaken the O—H bonds of interfacial H_2O molecules, decrease the energy barrier of H_2O dissociation, and accelerate the generation of adsorbed H_2 species, thus providing sufficient proton source for the NO_x^-RR. During the reduction reaction processes, the spark discharge non-thermal plasma can oxidize the N_2 in the air to NO_x, while the latter is further converted into the NO_x^- with the KOH solution.

27662098, 2026, 1, Downloaded from https://onlinelibrary.wiley.com/doi/10.1002/EXP.20240438 by CochraneChina, Wiley Online Library on [08/06/2026]. See the Terms and Conditions (https://onlinelibrary.wiley.com/terms-and-conditions) on Wiley Online Library for rules of use; OA articles are governed by the applicable Creative Commons License

TABLE 3 | Electrocatalysis, photocatalysis, or thermocatalysis coupling with plasma system for NH_3 synthesis.

Type	Catalyst	Electrolyte	NH_3 yield	FE (%)	Condition	Ref.
Electrocatalysis	Au/TiO_2	0.1 M HCl	1258.8 μmol g_{cat}^{-1} h^{-1}	8.11	−0.2 V versus RHE	[113]
	TiO_2/rGO	0.1 M Na_2SO_4	890 μmol g_{cat}^{-1} h^{-1}	3.3	−0.9 V versus RHE	[114]
	Ru SAs/N-C	0.05 M Na_2SO_4	7111.8 μmol g_{cat}^{-1} h^{-1}	29.6	−0.3 V versus RHE	[115]
	Cr_2O_3/CP	0.1 M Na_2SO_4	1488.2 μmol g_{cat}^{-1} h^{-1}	6.78	−0.9 V versus RHE	[116]
	B_4C/CPE	0.5 M H_2SO_4	1562.9 μmol g_{cat}^{-1} h^{-1}	15.95	−0.75 V versus RHE	[117]
Photocatalysis	CuCr-LDH	Water	73.5 μmol g_{cat}^{-1} h^{-1}	/	Full spectrum	[118]
	g-C_3N_4-V_N	Methanol	1240 μmol g_{cat}^{-1} h^{-1}	/	λ >420 nm	[119]
	Bi_5O_7Br	Water	1380 μmol g_{cat}^{-1} h^{-1}	/	λ > 400 nm	[120]
	BiOCl	Methanol	92.4 μmol g_{cat}^{-1} h^{-1}	/	Full spectrum	[121]
	MoS_2	Water	325 μmol g_{cat}^{-1} h^{-1}	/	λ > 420 nm	[122]
Thermocatalysis	$Co/BaCe_{3-x}N_yH_z$	/	10100 μmol g_{cat}^{-1} h^{-1}	/	673 K	[123]
	$Ru/Ca(NH_2)_2$	/	15800 μmol g_{cat}^{-1} h^{-1}	/	503 K	[124]
	Mn-LiH	/	11800 μmol g_{cat}^{-1} h^{-1}	/	650 K	[125]
	Co-LiH	/	4600 μmol g_{cat}^{-1} h^{-1}	/	573 K	[126]
	$Ru/BaTiO_3$	/	19360 μmol g_{cat}^{-1} h^{-1}	/	654 K	[127]
Plasma + electrocatalysis	$Cu_{10}Fe_1$-CFP	0.5 M Na_2SO_4	190.46 μmol cm_{cat}^{-2} h^{-1}	93.74	−0.53 V versus RHE	[103]
	Co_3O_4	1.0 M NaOH	2329.4 μmol cm_{cat}^{-2} h^{-1}	96.08	−0.8 V versus RHE	[102]
	N-MoS_2/VGs	0.1 M KOH	429.4 μmol cm_{cat}^{-2} h^{-1}	38.1	−0.53 V versus RHE	[128]
	Co SAs/N-C	0.1 M KOH	84.1 μmol cm_{cat}^{-2} h^{-1}	100	−0.33 V versus RHE	[129]
	Cu_2Pd/CBC	0.5 M KOH	115.1 μmol mg_{cat}^{-1} h^{-1}	93.79	−0.2 V versus RHE	[100]
	PtCu NP	1.5 M KOH	9.8 μmol mg_{cat}^{-1} h^{-1}	84.37	0 V versus RHE	[130]
Plasma + photocatalysis	/	Water	2.5 μmol min^{-1}	/	λ = 254 nm	[107]
	/	Water	1.17 μmol min^{-1}	/	/	[105]
	TiO_2	0.01 M H_2SO_4	/	/	λ = 319 nm	[106]
Plasma + thermocatalysis	Fe	/	4248 μmol g_{cat}^{-1} h^{-1}	/	/	[110]

The interfacial synergy between amorphous $Ni(OH)_x$ and Cu may also optimize the local micro-environment through electronic modulation, thereby realizing the adsorption of NO_x^- on the Cu surface, reducing the energy barrier towards hydrogenation step of key intermediates, and inhibiting the formation of side reactions. This work achieved the series connection of non-thermal plasma and interfacial H_2O dissociation-enhanced electrocatalyst (Figure 12C) for the first time, paving a new path for highly selective NH_3 synthesis. Besides, Wang et al. [80]. synthesized an Al_2O_3-supported transition-metal catalyst, which achieved the activation of N_2 to synthesize NH_3 at room temperature, by regulating the chemical properties of metal surface, especially the distribution of acid site intensity, and coupling with non-thermal plasma. The results show that the weak acid sites on the catalyst surface are positively correlated with the NH_3 synthesis rate (Figure 12D). Among different catalysts, the Ni/Al_2O_3 has higher concentration of weak acid sites compared with the Cu/Al_2O_3 and Fe/Al_2O_3, and its synthesis rate is more than twice that of pure Al_2O_3. This is because weak acid sites promote the formation as well as conversion of NH_2 intermediates, and accelerate the desorption of NH_3 simultaneously, while the strong acid sites lead to excessive adsorption of NH_3, thereby hindering the release of active sites. The work also reveals that surface chemical properties rather than physical structure dominate the plasma-catalytic synergistic effect. Although this new technology effectively avoids the high energy consumption problem of traditional H-B process, its plasma-catalytic synergistic mechanism still needs to be further optimized for improving energy efficiency. Liu et al. [103]. also prepared the highly dispersed Cu-Fe particles by the instantaneous thermal shock of Joule heating for NH_3 synthesis at ambient temperature and pressure, using the soluble nitrates produced by plasma activation of N_2 and O_2 in the air as the nitrogen source. The instantaneous high temperature and ultrafast cooling process can suppress the separation of alloy phases, thereby forming a homogeneous solid solution. As for the carbon fiber paper (CFP), it may accelerate the electron transfer, and prevent nanoparticles sintering through the confinement effect. Therefore, its uniformly dispersed Cu-Fe nanoparticles can expose more active sites than the naked counterparts (Figure 12E). Additionally, the free-standing catalyst can also inhibit the occurrence of competitive hydrogen evolution reaction, optimize the rate-controlling step (NO_3^- →

27662098, 2026, 1, Downloaded from https://onlinelibrary.wiley.com/doi/10.1002/EXP.20240438 by CochraneChina, Wiley Online Library on [08/06/2026]. See the Terms and Conditions (https://onlinelibrary.wiley.com/terms-and-conditions) on Wiley Online Library for rules of use; OA articles are governed by the applicable Creative Commons License

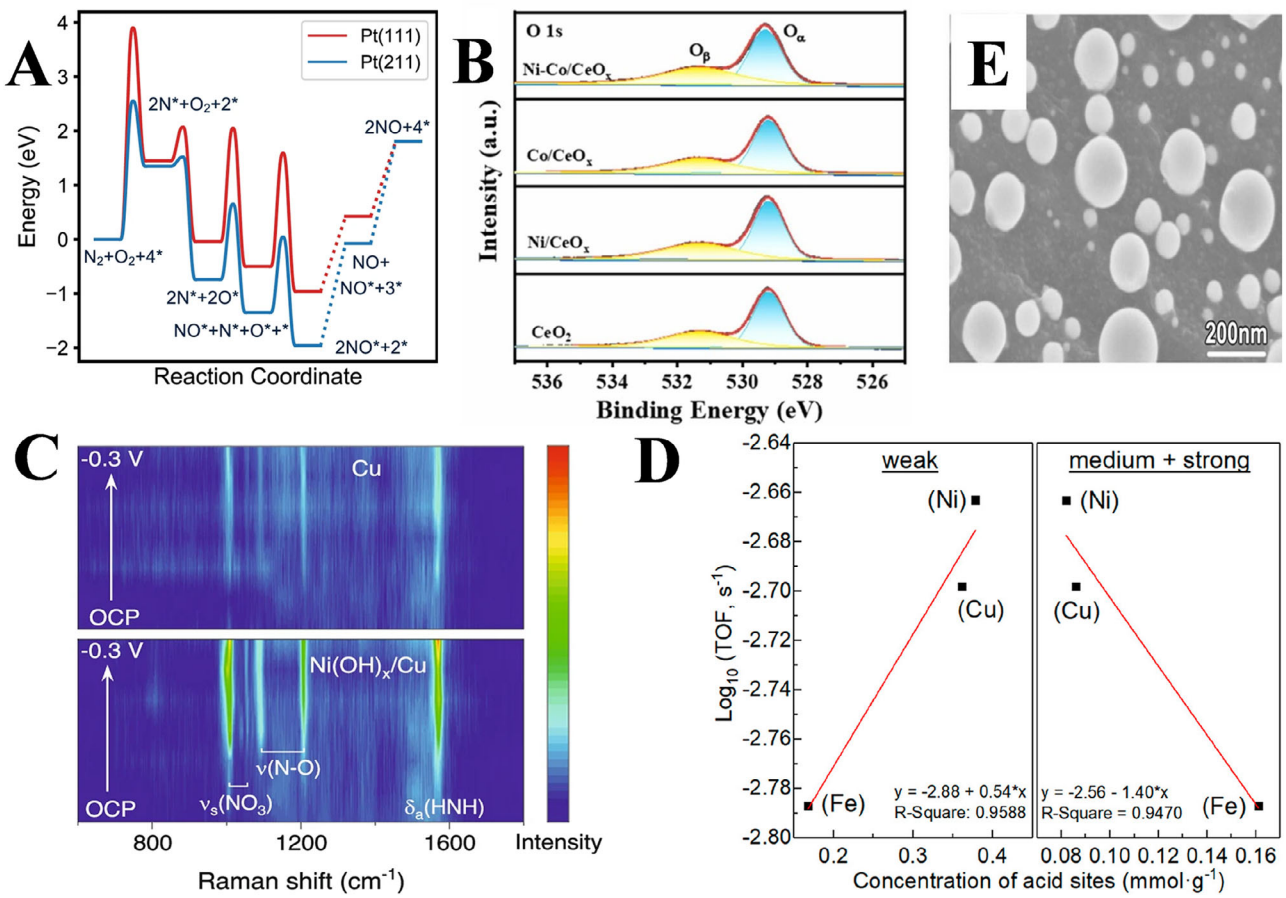


FIGURE 12 | (A) The DFT-reported potential energy surfaces for thermal N_2 oxidation on Pt (211) and Pt (111). Reproduced with permission Ref. [131]. (B) The high-resolution O 1 s spectra of CeO_2, Ni/CeO_x, Co/CeO_x, and Ni-Co/CeO_x. Reproduced with permission Ref. [132]. (C) Potential-dependent in situ Raman contour maps of Cu and Ni$(OH)_x$/Cu obtained during eNO_3^-RR in the potential range from 0.2 to −0.3 V versus reversible hydrogen electrode (vs. RHE). Reproduced with permission Ref. [101]. (D) Correlation between $\log_{10}$ (TOF, s^{-1}) with weak and medium + strong acid sites. Reproduced with permission Ref. [80]. (E) SEM image of $Cu_{10}Fe_1$-CFP. Reproduced with permission Ref. [103].

NO_2^-), accelerate mass transfer, and reduce intermediate product blockage. This work thus provides new ideas for the synthesis of green NH_3.

In the plasma-activated N_2 system, optimizing plasma parameters plays a key role in increasing efficiency of NH_3 synthesis. The results of laser-induced plasma studies confirm that unfocus length (UL) of laser significantly affects the plasma intensity and NH_3 yield. For example, when the UL is in the range of 0–1 mm, the plasma intensity is relatively high, with a NH_3 yield exceeding 28 μmol min^{-1}. However, the plasma weakens, and causes a significant decrease in NH_3 yield (~5.5 μmol min^{-1}), as the UL >2 mm [110]. For the DBD, nitrogen-rich atmosphere (N_2:H_2 = 3:1) is conducive to the dissociation of N_2 as the rate-controlling step, thereby improving the synthesis efficiency [44]. Increasing the driving frequency (52–65 kHz) can enlarge the micro-discharge density, thereby promoting N_2 dissociation and raising NH_3 yield, but if the frequency is too high (e.g., 68 kHz), the yield may also decrease slightly, due to the reaction equilibrium limitation [133]. In the double dielectric barrier discharge process, the highest NH_3 yield can be achieved at low power (5–6 W) and 450 K over a Ni catalyst. Nevertheless, excessive power will accelerate the decomposition of NH_3, because of local overheating, thereby reducing synthesis efficiency [134]. Based on above considerations, it can be inferred that precise control of plasma parameters is crucial to optimizing the plasma-activated NH_3 synthesis process. This requires striking a balance between enhancing key steps and avoiding disadvantages.

The synergistic effect of plasma and catalyst can activate N_2 to generate highly active free radicals. Combined with the synergistic interaction between the catalyst surfaces, it significantly reduces the activation energy of N_2 at room temperature and pressure, breaking through the thermodynamic limitations of traditional thermal catalytic pathways. In the meantime, the precise control of plasma parameters is the key to enhancing reaction kinetics and suppressing side reactions. Thus, the plasma coupled with catalytic technology offers a technical paradigm for the development of new catalysts in green NH_3 synthesis, and the exploration of synergistic optimization method of plasma and reactor structure in the future.

5 | Energy Consumption Analysis of Plasma-Assisted NH_3 Synthesis

Energy consumption is a comprehensive indicator that reflects the energy utilization rate of a process, and is also a summary

27662098, 2026, 1, Downloaded from https://onlinelibrary.wiley.com/doi/10.1002/EXP.20240438 by CochraneChina, Wiley Online Library on [08/06/2026]. See the Terms and Conditions (https://onlinelibrary.wiley.com/terms-and-conditions) on Wiley Online Library for rules of use; OA articles are governed by the applicable Creative Commons License

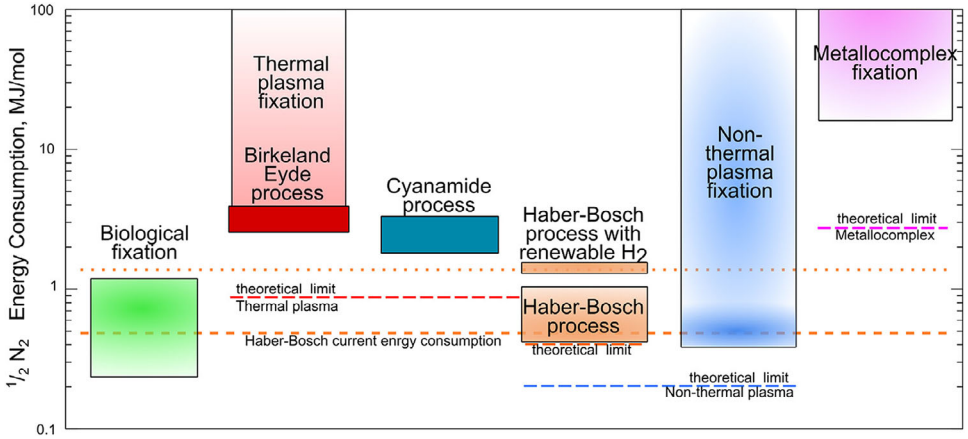


FIGURE 13 | A comparison for the energy consumption of N_2 fixation with different methods. Reproduced with permission Ref. [35].

indicator that ultimately reflects the economic benefits of industrial NH_3 synthesis [135]. Therefore, it is of interest to focus on the energy consumption of plasma-activated N_2 fixation. At present, the energy consumption of traditional H-B process has reached a bottleneck, that is, 0.48 MJ $mol_{NH_3}^{-1}$ [136]. Contrarily, the energy consumption of plasma-assisted NH_3 synthesis is still expected to be further reduced [35]. As illustrated in Figure 13, although the H-B process still owns the lowest energy consumption, it is already close to the theoretical limit. In comparison, the non-thermal plasma-assisted NH_3 synthesis has a larger room for energy efficiency improvement than the H-B process, showing a greater competitive advantage. In particular, the electrochemical NH_3 synthesis technology has attracted widespread attention, with the rapid development of renewable energy and the rise of distributed energy system, because it could operate under mild conditions and be coupled with green electricity resources. Nevertheless, the energy consumption of H-B process is far lower than that of most electrochemical synthesis pathways, resulting from nearly a century of process optimizations and scale economies. For example, the energy consumption of electrochemical method based on the PEM technology is as large as 98.1–220.7 MJ mol^{-1}, while its FE is only 0.16%–0.36%, reflecting that the NRR faces severe kinetic barriers and fierce competition from side reactions [137]. At present, some electrochemical pathways have made significant progress in energy consumption, and shown great development potential. In this regard, the energy consumption of mixed conducting electrolyte route is about 7.97–69.89 MJ mol^{-1}, which is far superior to that of PEM system [138]. More impressively, the alkaline exchange membrane (AEM) system further reduces the energy consumption of electrochemical NH_3 synthesis to 0.858–31.88 MJ mol^{-1} [139]. However, the limit still exists, that is, although the FE of AEM technology can reach 41% in the initial stage, it quickly declines to single-digit level within a few hours. Such rapid performance decay reveals that the electrochemical NH_3 synthesis still faces huge challenges in the long-term stability. In the future, it is necessary to maintain high FE while taking into account the stability of electrochemical NH_3 synthesis, as a powerful alternative to the conventional H-B process. A brief summary for the energy consumption of plasma-enhanced N_2 fixation is listed in Table 4. In general, the plasma-based N_2 fixation can be described in the following two pathways.

The pathway 1 is $N_2 \rightarrow NH_3$. Over the past decade, researchers have been working on the plasma-assisted reduction of N_2 by H_2 using diverse catalysts for continuous improvement in production efficiency and energy consumption of NH_3 synthesis. Representatively, Patil et al. [69]. screened 16 different transition metals as well as oxides, and discussed their effects on the DBD plasma-catalyzed synthesis of NH_3 in detail. By optimizing the feed ratio, specific energy input, reaction temperature, metal loading and gas flow rate, a low energy consumption of 32 MJ $mol_{NH_3}^{-1}$ was achieved. The results demonstrated that the matching between plasma discharge parameter and catalyst was also very critical, besides the catalyst screening. Kim et al. [140]. happen to be coincident with the Ptail's findings, and realized a low energy consumption of 28.01 MJ $mol_{NH_3}^{-1}$ in the nanosecond pulsed-filled-bed reactor with a Ru(2)-Mg(5)/γ-Al_2O_3 catalyst accompanied by a feed ratio of N_2:H_2 = 4:1 at 300°C and atmospheric pressure. Through the understanding of conventional H-B process and above-mentioned plasma routes, it can be known that the one-step synthesis of NH_3 using N_2 and H_2 as feedstock involves an additional H_2 production step, and thus requires a lot of energy consumption. In contrast, non-hydrogen reduction N_2 fixation technology not only avoids this energy-intensive step, but also simplifies the synthetic procedure.

The pathway 2 is $N_2 \rightarrow NO_x^- \rightarrow NH_3$. In addition to the direct one-step synthesis of NH_3 via the NRR with H_2, N_2 can also be oxidized firstly to reactive NO_x^- species by O_2, and then further reduced to NH_3. In this regard, Liang et al. [141]. proposed a cascade connected N_2 fixation strategy with the DBD plasma oxidation and electrocatalytic reduction (pNF-eNO_x^-RR), which could complete the NH_3 synthesis process through a two-step reactions. For instance, N_2 is oxidized to be NO_x^- by the plasma, while the latter is subsequently absorbed by the KOH solution, and electro-reduced to NH_3. This process may achieve a high NH_3 yield of 16.21 mg h^{-1} with an energy efficiency of 2.08%, and a total energy consumption of 18.36 MJ $mol_{NH_3}^{-1}$ that is much lower than that of the plasma-activated proton-conducting solid-oxide electrolyzer (605 MJ $mol_{NH_3}^{-1}$) [99]. Zheng et al. [128]. also connected the plasma in series with a dual electrocatalytic electrolyzer, and developed a matching catalyst, that is, the defective N-doped molybdenum sulfide nanosheets loaded on vertical graphene arrays (N-MoS_2/VGs), thus achieving a low

27662098, 2026, 1, Downloaded from https://onlinelibrary.wiley.com/doi/10.1002/EXP.20240438 by CochraneChina, Wiley Online Library on [08/06/2026]. See the Terms and Conditions (https://onlinelibrary.wiley.com/terms-and-conditions) on Wiley Online Library for rules of use; OA articles are governed by the applicable Creative Commons License

TABLE 4 | A summary for the energy consumption of reported plasma-catalyzed NH_3 synthesis.

Pathway	Plasma type	Catalyst	Gas	Energy consumption MJ $mol_{NO_x}^{-1}$	Energy consumption MJ $mol_{NH_3}^{-1}$	Ref.
H-B Plasma	/	Fe	N_2, H_2	/	0.48	[136]
	DBD	/	N_2, H_2	/	59	[104]
	DBD	Ni/LaOF	N_2, H_2	/	22.6	[51]
	DBD	Ni/Al_2O_3	N_2, H_2	/	20.82	[80]
	RF	Ni-MOF-74	N_2, H_2	/	265	[54]
	RF	Au wire	N_2, H_2	/	322.7	[106]
	MW	/	N_2, H_2	/	1532.8	[61]
Electrocatalysis	/	Pt	N_2, H_2	/	98.1–220.7	[137]
	/	Perovskite	Air	/	7.97–69.89	[138]
	/	Pt, Fe, Ni, FeNi	Air	/	0.858–31.88	[139]
Plasma electrolysis	CD	Cu_2O nanowire	Air	8.604	14.076	[63]
	Jet	/	N_2	/	138.96	[107]
	DBD	/	Air	1.06	15.49	[37]
	Jet	Co_3O_4	Air	40.248	>40.248	[62]
	GA	Co SAs/N-C	N_2/O_2	2.4	3.18	[108]
	GAD + MW-PM	PtCu NP	Air	/	33.78	[109]

energy consumption of 2.4 MJ $mol_{NH_3}^{-1}$. Although their energy consumption is higher than that of the traditional H-B process, the pNF-eNO_x^-RR system can still provide an alternative route for the development of decentralized NH_3 synthesis industry, considering that the H-B process is only economically feasible in large-scale production.

Based on the understanding of development status in plasma-catalyzed NH_3 synthesis technology, one may infer that although its energy consumption is inferior to that of the H-B industry, it has more obvious advantages in compatibility with renewable energy, such as solar, wind and tidal resources [142–145]. Meanwhile, its operating conditions are also milder than those of conventional method. Therefore, it may be a feasible and competitive alterative with good development and application potential for remote areas or small-scale, decentralized NH_3 production.

6 | Conclusions and Outlook

In summary, we review the current status of research on the plasma-enhanced NH_3 synthesis, while comprehensively sorting out the problems existing in the synthetic process. Up to date, a variety of plasmas have been used, showing broad application prospects in NH_3 synthesis. The future research focus of plasma-enhanced NH_3 synthesis will mainly include the following aspects.

1. The optimization of reaction system: the plasma activation process consumes a large amount of energy, and produces active substances with a short lifetime, thus it is necessary to optimize the reactor design for improving the activation efficiency of plasma on N_2. Currently, the DBD plasma is the most commonly used discharge strategy in the NH_3 synthesis process, and correspondingly various DBD reactors, including fixed bed, packed bed, and fluidized, etc., are developed. Optimizing key parameters, such as electrode type and shape, discharge gap and type, dielectric constant, and gas dilution, can effectively reduce the energy cost of NH_3 synthesis. In addition, the gas flow field inside the reaction device must be rationally designed, so that the raw materials can be evenly distributed in the plasma, thereby increasing the probability of collision between the reaction gas and high-energy particles. Installing the gas distributor along with optimizing the shape as well as size of the reactor can also promote gas turbulence, and thus enhance mass transfer. Based on these measures, the active substances produced by N_2 activation can be fully utilized, and meanwhile the loss of energy and substances may be effectively avoided, too.
2. The development of highly synergistically active catalysts, and the usage of aprotic solvent are key to promoting N_2 dissociation and adsorption reactions of surface-active species as well. Among them, the catalyst selection in plasma-assisted NH_3 synthesis, including catalyst precursor, support and additive, is particularly important. First, the designed catalyst should be able to promote the generation of active N_2 and H_2 species in the plasma, and accelerate their reaction, thereby increasing the NH_3 yield. For instance, the catalyst surface should have a suitable electronic structure to facilitate the adsorption, activation and conversion of active species. Secondly, one of the bottlenecks hindering the industrialization of plasma-enhanced NH_3 synthesis is the poor interaction between plasma and catalyst, which

27662098, 2026, 1, Downloaded from https://onlinelibrary.wiley.com/doi/10.1002/EXP.20240438 by CochraneChina, Wiley Online Library on [08/06/2026]. See the Terms and Conditions (https://onlinelibrary.wiley.com/terms-and-conditions) on Wiley Online Library for rules of use; OA articles are governed by the applicable Creative Commons License

has not been fully resolved. Currently, the combination of Co-Ni/MOF-74 catalyst with DBD plasma has only achieved a NH_3 yield of ~43.48 μmol g^{-1} min^{-1} at ambient temperature and pressure. This requires in-depth research on their synergistic mechanism, and continuous optimization of the catalyst's property and structure based on the plasma discharge mode and equipment parameters, etc. These help to achieve a successful match between catalyst and plasma, thereby improving the energy efficiency and production rate of NH_3 synthesis. Therefore, it is necessary to explore more advanced in situ characterization techniques, such as infrared, synchrotron radiation X-ray absorption, laser-induced fluorescence and laser-scattering spectroscopies, to monitor the activation degree of N_2, the generation and consumption of intermediates, and the synthesis rate of NH_3. Real-time analysis of the above parameters is conducive to investigating the influence of catalyst on the physicochemical property of plasma, thereby revealing the synergistic mechanism of plasma-catalyzed NH_3 synthesis.

3. In-depth study of the NRR mechanism is of great significance to improving NH_3 yield too, which can offer theoretical guide for the selection of raw materials and the optimization of reaction conditions. The investigation of reaction mechanism is helpful to understand all aspects of the NRR from its source. Specifically, there is still controversy over the specific pathway and rate-determining step of NRR process. At the same time, the synergistic reaction mechanism of plasma catalysis needs further in-depth study. In the future, researchers should establish a more accurate kinetic model of plasma-activated N_2 fixation. After that, the reaction mechanism of plasma-activated NRR can be investigated in depth by using quantum chemical calculations and molecular dynamics simulations, including the N_2 dissociation, free radical generation, intermediate product, and NH_3 desorption, etc. This is of vital importance in guiding specific experiments.

4. Combining plasma with other technologies, including electrocatalysis, photocatalysis, and thermocatalysis, etc., can not only give full play to the advantages of each technology, but also overcome the limitations of a single technology. For example, a high NH_3 yield of 2329.4 μmol h^{-1} cm^{-2} with a FE of 96.08% can be achieved in the electrocatalytic system, through the integration of plasma with Co_3O_4 catalyst. But as one of very important means to significantly reduce the energy consumption, and elevate the NRR efficiency, coupling of plasma technology and other catalytic technologies still has much room for improvement. This also requires continuous pursuit of new N_2 fixation technologies with high economic benefit and efficiency. In this regard, it is recommended to closely combine the plasma reactor with other catalytic reactors by constructing an integrated reaction system, thereby reducing energy and product losses in the intermediate transmission process. Correspondingly, theoretical studies on the plasma-catalyzed coupling reactions should also be carried out. For example, the formation mechanism and charge transfer process of active species on the electrode surface during the plasma-assisted electrocatalysis, as well as the energy transformation and synergistic mechanism between different plasma and photo/thermocatalysis might be worth further investigation. The above researches can offer a theoretical basis for the development of new and efficient integration technologies, thereby promoting the industrialization of plasma-catalyzed NH_3 synthesis.

Acknowledgments

The authors are grateful for financial support from the National Natural Science Foundation of China [Nos. 22178360, 22378400 and 51804132], State Key Laboratory of Chemical Engineering, Tsinghua University [No. SKL-ChE-23A02], "Chunhui Plan" Cooperative Scientific Research Project of Ministry of Education [No. HZKY20220097-202200280], and High-End Foreign Experts Program [No. G2023199001L].

Conflicts of Interest

The authors declare no conflicts of interest.

Data Availability Statement

The data that support the findings of this study are available on request from the corresponding author. The data are not publicly available due to privacy or ethical restrictions.

References

1. X. Fu, A. Xu, J. B. Pedersen, et al., "Phenol as Proton Shuttle and Buffer for Lithium-Mediated Ammonia Electrosynthesis," *Nature Communications* 15 (2024): 2417, https://doi.org/10.1038/s41467-024-46803-w.

2. S. J. Zheng, X. Y. Dong, H. Chen, R. W. Huang, J. Cai, and S. Q. Zang, "Unveiling Ionized Interfacial Water-Induced Localized H* Enrichment for Electrocatalytic Nitrate Reduction," *Angewandte Chemie, International Edition* 64 (2024): e202413033, https://doi.org/10.1002/anie.202413033.

3. H. Chen, L. Liu, X. H. Ma, et al., "Atomically Precise Silver-Based Bimetallic Clusters for Electrocatalytic Urea Synthesis," *National Science Review* 12 (2025): nwae440, https://doi.org/10.1093/nsr/nwae440.

4. Y. Wei, J. Huang, H. Chen, et al., "Electrocatalytic Nitrate Reduction on Metallic CoNi-Terminated Catalyst With Industrial-Level Current Density in Neutral Medium," *Advanced Materials* 36 (2024): 2404774, https://doi.org/10.1002/adma.202404774.

5. L. Liu, S. J. Zheng, H. Chen, J. Cai, and S. Q. Zang, "Tandem Nitrate-to-Ammonia Conversion on Atomically Precise Silver Nanocluster/MXene Electrocatalyst," *Angewandte Chemie, International Edition* 63 (2024): e202316910, https://doi.org/10.1002/anie.202316910.

6. D. R. MacFarlane, P. V. Cherepanov, J. Choi, et al., "A Roadmap to the Ammonia Economy," *Joule* 4 (2020): 1186–1205, https://doi.org/10.1016/j.joule.2020.04.004.

7. C. Smith, A. K. Hill, and L. Torrente-Murciano, "Current and Future Role of Haber–Bosch Ammonia in a Carbon-Free Energy Landscape," *Energy & Environmental Science* 13 (2020): 331–344, https://doi.org/10.1039/C9EE02873K.

8. G. F. Han, F. Li, Z. W. Chen, et al., "Mechanochemistry for Ammonia Synthesis Under Mild Conditions," *Nature Nanotechnology* 16 (2020): 325–330, https://doi.org/10.1038/s41565-020-00809-9.

9. X. Fu, V. A. Niemann, Y. Zhou, et al., "Calcium-Mediated Nitrogen Reduction for Electrochemical Ammonia Synthesis," *Nature Materials* 23 (2024): 101–107, https://doi.org/10.1038/s41563-023-01702-1.

10. X. Zhu, S. Mou, Q. Peng, et al., "Aqueous Electrocatalytic N_2 Reduction for Ambient NH_3 Synthesis: Recent Advances in Catalyst Development and Performance Improvement," *Journal of Materials Chemistry A* 8 (2020): 1545–1556, https://doi.org/10.1039/C9TA13044F.

11. C. Cui, Y. Jia, H. Zhang, L. Geng, and Z. Luo, "Plasma-Assisted Chain Reactions of Rh_3+ Clusters With Dinitrogen: N≡N Bond Dissociation,"

27662098, 2026, 1, Downloaded from https://onlinelibrary.wiley.com/doi/10.1002/EXP.20240438 by CochraneChina, Wiley Online Library on [08/06/2026]. See the Terms and Conditions (https://onlinelibrary.wiley.com/terms-and-conditions) on Wiley Online Library for rules of use; OA articles are governed by the applicable Creative Commons License

Journal of Physical Chemistry Letters 11 (2020): 8222–8230, https://doi.org/10.1021/acs.jpclett.0c02218.

12. X. Fu, J. B. Pedersen, Y. Zhou, et al., "Continuous-Flow Electrosynthesis of Ammonia by Nitrogen Reduction and Hydrogen Oxidation," *Science* 379 (2023): 707–712, https://doi.org/10.1126/science.adf4403.

13. S. Li, Y. Zhou, X. Fu, et al., "Long-Term Continuous Ammonia Electrosynthesis," *Nature* 629 (2024): 92–97, https://doi.org/10.1038/s41586-024-07276-5.

14. T. S. Bui, E. C. Lovell, R. Daiyan, and R. Amal, "Defective Metal Oxides: Lessons From CO_2RR and Applications in NO_XRR," *Advanced Materials* 35 (2023): 2205814, https://doi.org/10.1002/adma.202205814.

15. T. N. Ye, S. W. Park, Y. Lu, et al., "Vacancy-Enabled N_2 Activation for Ammonia Synthesis on an Ni-Loaded Catalyst," *Nature* 583 (2020): 391–395, https://doi.org/10.1038/s41586-020-2464-9.

16. Y. Zhai, Z. Zhu, C. Zhu, et al., "Single-Atom Catalysts Boost Nitrogen Electroreduction Reaction," *Materials Today* 38 (2020): 99–113, https://doi.org/10.1016/j.mattod.2020.03.022.

17. Y. Wan, J. Xu, and R. Lv, "Heterogeneous Electrocatalysts Design for Nitrogen Reduction Reaction Under Ambient Conditions," *Materials Today* 27 (2019): 69–90, https://doi.org/10.1016/j.mattod.2019.03.002.

18. Q. Huang, B. Xia, M. Li, H. Guan, M. Antonietti, and S. Chen, "Single-Zinc Vacancy Unlocks High-Rate H_2O_2 Electrosynthesis From Mixed Dioxygen Beyond Le Chatelier Principle," *Nature Communications* 15 (2024): 4157, https://doi.org/10.1038/s41467-024-48256-7.

19. F. Zhu, J. Ge, Y. Gao, et al., "Molten Salt Electro-Preparation of Graphitic Carbons," *Exploration* 3 (2023): 20210186, https://doi.org/10.1002/EXP.20210186.

20. A. Abu Hajer, D. A. Daramola, and J. P. Trembly, "Carbon Dioxide Reduction in Solid Oxide Electrolyzer Cells Utilizing Nickel Bimetallic Alloys Infiltrated Into Gd0.1Ce0.9O1.95 (GDC10) Scaffolds," *Electrochimica Acta* 485 (2024): 144052.

21. M. Wang, J. Ma, Z. Shang, et al., "Advances in Ambient Selective Electrohydrogenation of Nitrogen to Ammonia: Strategies to Strengthen Nitrogen Chemisorption," *Journal of Materials Chemistry A* 11 (2023): 3871–3887, https://doi.org/10.1039/D2TA07763A.

22. L. H. Mou, Z. Y. Li, and S. G. He, "Recent Progress in Dinitrogen Activation by Gas-Phase Metal Species," *Journal of Physical Chemistry Letters* 13 (2022): 4159–4169, https://doi.org/10.1021/acs.jpclett.2c00850.

23. L. H. Mou, G. D. Jiang, Z. Y. Li, and S. G. He, "Activation of Dinitrogen by Gas-Phase Species," *Chinese Journal of Chemical Physics* 33 (2020): 507–520, https://doi.org/10.1063/1674-0068/cjcp2008141.

24. Y. Ren, C. Yu, X. Tan, et al., "Strategies to Activate Inert Nitrogen Molecules for Efficient Ammonia Electrosynthesis: Current Status, Challenges, and Perspectives," *Energy & Environmental Science* 15 (2022): 2776–2805, https://doi.org/10.1039/D2EE00358A.

25. M. Liang, X. Shao, and H. Lee, "Recent Developments of Dual Single-Atom Catalysts for Nitrogen Reduction Reaction," *Chemistry – European Journal* 30 (2024): e202302843, https://doi.org/10.1002/chem.202302843.

26. X. Xue, R. Chen, C. Yan, et al., "Review on Photocatalytic and Electrocatalytic Artificial Nitrogen Fixation for Ammonia Synthesis at Mild Conditions: Advances, Challenges and Perspectives," *Nano Research* 12 (2019): 1229–1249, https://doi.org/10.1007/s12274-018-2268-5.

27. S. Zhang, Y. Zhao, R. Shi, G. I. N. Waterhouse, and T. Zhang, "Photocatalytic Ammonia Synthesis: Recent Progress and Future," *EnergyChem* 1 (2019): 100013, https://doi.org/10.1016/j.enchem.2019.100013.

28. J. Deng, J. A. Iñiguez, and C. Liu, "Electrocatalytic Nitrogen Reduction at Low Temperature," *Joule* 2 (2018): 846–856, https://doi.org/10.1016/j.joule.2018.04.014.

29. V. Kyriakou, I. Garagounis, E. Vasileiou, A. Vourros, and M. Stoukides, "Progress in the Electrochemical Synthesis of Ammonia," *Catalysis Today* 286 (2017): 2–13, https://doi.org/10.1016/j.cattod.2016.06.014.

30. P. Li, Y. Liu, M. A. Mushtaq, and D. Yan, "Recent Progress in Ammonia Synthesis Based on Photoelectrocatalysis," *Inorganic Chemistry Frontiers* 10 (2023): 4650–4667, https://doi.org/10.1039/D3QI00683B.

31. Y. Ren, S. Li, C. Yu, et al., "NH_3 Electrosynthesis From N_2 Molecules: Progresses, Challenges, and Future Perspectives," *Journal of the American Chemical Society* 146 (2024): 6409–6421, https://doi.org/10.1021/jacs.3c11676.

32. L. R. Winter and J. G. Chen, "N_2 Fixation by Plasma-Activated Processes," *Joule* 5 (2021): 300–315, https://doi.org/10.1016/j.joule.2020.11.009.

33. A. Klimek and D. G. Piercey, "Nitrogen Fixation via Plasma-Assisted Processes: Mechanisms, Applications, and Comparative Analysis—A Comprehensive Review," *Processes* 12 (2024): 786, https://doi.org/10.3390/pr12040786.

34. P. Peng, P. Chen, C. Schiappacasse, et al., "A Review on the Non-Thermal Plasma-Assisted Ammonia Synthesis Technologies," *Journal of Cleaner Production* 177 (2018): 597–609, https://doi.org/10.1016/j.jclepro.2017.12.229.

35. N. Cherkasov, A. O. Ibhadon, and P. Fitzpatrick, "A Review of the Existing and Alternative Methods for Greener Nitrogen Fixation," *Chemical Engineering Processes* 90 (2015): 24–33, https://doi.org/10.1016/j.cep.2015.02.004.

36. M. L. Carreon, "Plasma Catalytic Ammonia Synthesis: State of the Art and Future Directions," *Journal of Physics D: Applied Physics* 52 (2019): 483001, https://doi.org/10.1088/1361-6463/ab3b2c.

37. M. Yamazaki and K. Sasaki, "Efficient Vibrational Excitation of Molecular Nitrogen in Low-Pressure Plasma With Ultralow Electron Temperature," *Plasma Sources Science and Technology* 31 (2022): 094004, https://doi.org/10.1088/1361-6595/ac8b2f.

38. A. Denra, S. Saud, D. B. Nguyen, et al., "Nitrogen Fixation by Rotational Gliding Arc Plasma at Surrounding Conditions," *Journal of Cleaner Production* 436 (2024): 140618, https://doi.org/10.1016/j.jclepro.2024.140618.

39. K. H. R. Rouwenhorst, Y. Engelmann, K. van't Veer, R. S. Postma, A. Bogaerts, and L. Lefferts, "Plasma-Driven Catalysis: Green Ammonia Synthesis With Intermittent Electricity," *Green Chemistry* 22 (2020): 6258–6287, https://doi.org/10.1039/D0GC02058C.

40. S. Van Alphen, V. Vermeiren, T. Butterworth, D. C. M. van den Bekerom, G. J. van Rooij, and A. Bogaerts, "Power Pulsing To Maximize Vibrational Excitation Efficiency in N_2 Microwave Plasma: A Combined Experimental and Computational Study," *Journal of Physical Chemistry C* 124 (2019): 1765–1779, https://doi.org/10.1021/acs.jpcc.9b06053.

41. N. Gatti, S. Ponduri, F. J. J. Peeters, et al., "Preferential Vibrational Excitation in Microwave Nitrogen Plasma Assessed by Raman Scattering," *Plasma Sources Science and Technology* 27 (2018): 055006, https://doi.org/10.1088/1361-6595/aabd60.

42. P. Mehta, P. Barboun, F. A. Herrera, et al., "Overcoming Ammonia Synthesis Scaling Relations With Plasma-Enabled Catalysis," *Nature Catalysis* 1 (2018): 269–275, https://doi.org/10.1038/s41929-018-0045-1.

43. A. Vojvodic, A. J. Medford, F. Studt, et al., "Exploring the Limits: A Low-Pressure, Low-Temperature Haber–Bosch Process," *Chemical Physics Letters* 598 (2014): 108–112, https://doi.org/10.1016/j.cplett.2014.03.003.

44. L. R. Winter, B. Ashford, J. Hong, A. B. Murphy, and J. G. Chen, "Identifying Surface Reaction Intermediates in Plasma Catalytic Ammonia Synthesis," *ACS Catalysis* 10 (2020): 14763–14774, https://doi.org/10.1021/acscatal.0c03166.

45. K. H. R. Rouwenhorst, H. G. B. Burbach, D. W. Vogel, J. Núñez Paulí, B. Geerdink, and L. Lefferts, "Plasma-Catalytic Ammonia Synthesis Beyond Thermal Equilibrium on Ru-Based Catalysts in Non-Thermal Plasma," *Catalysis Science & Technology* 11 (2021): 2834–2843, https://doi.org/10.1039/D0CY02189J.

27662098, 2026, 1, Downloaded from https://onlinelibrary.wiley.com/doi/10.1002/EXP.20240438 by CochraneChina, Wiley Online Library on [08/06/2026]. See the Terms and Conditions (https://onlinelibrary.wiley.com/terms-and-conditions) on Wiley Online Library for rules of use; OA articles are governed by the applicable Creative Commons License

46. A. J. Medford, A. Vojvodic, J. S. Hummelshøj, et al., "From the Sabatier Principle to a Predictive Theory of Transition-Metal Heterogeneous Catalysis," *Journal of Catalysis* 328 (2015): 36–42, https://doi.org/10.1016/j.jcat.2014.12.033.

47. X. Zeng, S. Zhang, X. Hu, C. Zhang, K. Ostrikov, and T. Shao, "Recent Advances in Plasma-Enabled Ammonia Synthesis: State-of-the-Art, Challenges, and Outlook," *Faraday Discussions* 243 (2023): 473–491, https://doi.org/10.1039/D3FD00006K.

48. H. Patel, R. K. Sharma, V. Kyriakou, et al., "Plasma-Activated Electrolysis for Cogeneration of Nitric Oxide and Hydrogen From Water and Nitrogen," *ACS Energy Letters* 4 (2019): 2091–2095, https://doi.org/10.1021/acsenergylett.9b01517.

49. Y. Setsuhara, "Low-Temperature Atmospheric-Pressure Plasma Sources for Plasma Medicine," *Archives of Biochemistry and Biophysics* 605 (2016): 3–10, https://doi.org/10.1016/j.abb.2016.04.009.

50. P. Mehta, P. Barboun, D. B. Go, J. C. Hicks, and W. F. Schneider, "Catalysis Enabled by Plasma Activation of Strong Chemical Bonds: A Review," *ACS Energy Letters* 4 (2019): 1115–1133, https://doi.org/10.1021/acsenergylett.9b00263.

51. K. Li, S. Chen, H. Wang, and F. Wang, "Plasma-Assisted Ammonia Synthesis Over Ni/LaOF: Dual Active Centers Consisting of Oxygen Vacancies and Ni," *Applied Catalysis A: General* 650 (2023): 118983, https://doi.org/10.1016/j.apcata.2022.118983.

52. K. Li, S. Chen, M. Li, L. Liu, Y. Li, and F. Wang, "Plasma-Catalyzed Ammonia Synthesis Over $La(OH)_3$ Catalyst: Effects of Basic Sites, Oxygen Vacancies, and H_2 Plasma Treatment," *International Journal of Hydrogen Energy* 59 (2024): 1287–1296, https://doi.org/10.1016/j.ijhydene.2024.02.123.

53. J. Chen, T. Tang, X. Wu, et al., "Unlocking Efficient Synergistic Plasma-Catalyst Ammonia Synthesis: System Optimization and Catalyst Support Screening," *Energy Fuels* 38 (2024): 10345–10356, https://doi.org/10.1021/acs.energyfuels.4c00702.

54. J. Shah, T. Wu, J. Lucero, M. A. Carreon, and M. L. Carreon, "Nonthermal Plasma Synthesis of Ammonia Over Ni-MOF-74," *ACS Sustainable Chemistry & Engineering* 7 (2018): 377–383, https://doi.org/10.1021/acssuschemeng.8b03705.

55. Y. Liu, X. Xu, Q. Song, et al., "Co-Ni/MOF-74 Catalyst Packed-Bed DBD Plasma for Ammonia Synthesis," *Plasma Processes and Polymers* 21 (2023): 2300086, https://doi.org/10.1002/ppap.202300086.

56. J. Feng, P. Ning, K. Li, et al., "One-Step Synthesis of Ammonia Directly From Wet Air/N_2 by Plasma Combined With a γ-Al_2O_3 Catalyst," *ACS Sustainable Chemistry & Engineering* 11 (2023): 804–814, https://doi.org/10.1021/acssuschemeng.2c06706.

57. Y. Zhang, S. Li, B. Qiu, S. Chen, H. Chen, and X. Fan, "MgAl Layered Double Hydroxide (LDH) for Promoting Ammonia Synthesis in Non-Thermal Plasma: Role of Surface Oxygen Vacancy," *Chemical Engineering Processes* 195 (2024): 109608, https://doi.org/10.1016/j.cep.2023.109608.

58. T. Zhang, R. Zhou, S. Zhang, et al., "Sustainable Ammonia Synthesis From Nitrogen and Water by One-Step Plasma Catalysis," *Energy & Environmental Materials* 6 (2022): e12344, https://doi.org/10.1002/eem2.12344.

59. X. Li, Y. Jiao, Y. Cui, et al., "Synergistic Catalysis of the Synthesis of Ammonia With Co-Based Catalysts and Plasma: From Nanoparticles to a Single Atom," *ACS Applied Materials & Interfaces* 13 (2021): 52498–52507, https://doi.org/10.1021/acsami.1c12695.

60. Y. Li, S. Chen, K. Li, et al., "Plasma-Assisted Ammonia Synthesis Over La_2O_3 Modified by RF Discharge: Effect of Oxygen Vacancies on N_2 Adsorption and Associative Mechanism," *ACS Sustainable Chemistry & Engineering* 12 (2024): 11728–11738, https://doi.org/10.1021/acssuschemeng.4c03610.

61. K. H. R. Rouwenhorst, S. Mani, and L. Lefferts, "Improving the Energy Yield of Plasma-Based Ammonia Synthesis With In Situ Adsorption," *ACS Sustainable Chemistry & Engineering* 10 (2022): 1994–2000, https://doi.org/10.1021/acssuschemeng.1c08467.

62. F. Tochikubo and A. Komuro, "Review of Numerical Simulation of Atmospheric-Pressure Non-Equilibrium Plasmas: Streamer Discharges and Glow Discharges," *The Japanese Journal of Applied Physics* 60 (2021): 040501, https://doi.org/10.35848/1347-4065/abe6e2.

63. J. Nakajima and H. Sekiguchi, "Synthesis of Ammonia Using Microwave Discharge at Atmospheric Pressure," *Thin Solid Films* 516 (2008): 4446–4451, https://doi.org/10.1016/j.tsf.2007.10.053.

64. S. Brown, S. Ahmat Ibrahim, B. R. Robinson, et al., "Ambient Carbon-Neutral Ammonia Generation via a Cyclic Microwave Plasma Process," *ACS Applied Materials & Interfaces* 15 (2023): 23255–23264, https://doi.org/10.1021/acsami.3c02508.

65. X. Bai, S. Tiwari, B. Robinson, C. Killmer, L. Li, and J. Hu, "Microwave Catalytic Synthesis of Ammonia From Methane and Nitrogen," *Catalysis Science & Technology* 8 (2018): 6302–6305, https://doi.org/10.1039/C8CY01355A.

66. B. Indumathy, J. Ananthanarasimhan, L. Rao, S. Yugeswaran, and P. V. Ananthapadmanabhan, "Catalyst-Free Production of Ammonia by Means of Interaction Between a Gliding Arc Plasma and Water Surface," *Journal of Physics D: Applied Physics* 55 (2022): 395501, https://doi.org/10.1088/1361-6463/ac7b52.

67. X. Gong, L. Feng, S. Tan, et al., "In Situ Synthesis and Measurement of Ammonia From Nitrogen by Nanoelectrospray-Based Corona Discharge Coupled With Mass Spectrometry," *ACS Energy Letters* 9 (2024): 2153–2161, https://doi.org/10.1021/acsenergylett.4c00427.

68. V. D. Rusanov, A. A. Fridman, and G. V. E. Sholin, "The Physics of a Chemically Active Plasma With Nonequilibrium Vibrational Excitation of Molecules," *Soviet Physics Uspekhi* 24 (1981): 447–474, https://doi.org/10.1070/PU1981v024n06ABEH004884.

69. B. S. Patil, Q. Wang, V. Hessel, and J. Lang, "Plasma N_2-Fixation: 1900–2014," *Catalysis Today* 256 (2015): 49–66, https://doi.org/10.1016/j.cattod.2015.05.005.

70. S. Li, J. Medrano Jimenez, V. Hessel, and F. Gallucci, "Recent Progress of Plasma-Assisted Nitrogen Fixation Research: A Review," *Processes* 6 (2018): 248, https://doi.org/10.3390/pr6120248.

71. M. Bai, Z. Zhang, M. Bai, X. Bai, and H. Gao, "Synthesis of Ammonia Using CH_4/N_2 Plasmas Based on Micro-Gap Discharge Under Environmentally Friendly Condition," *Plasma Chemistry and Plasma Processing* 28 (2008): 405–414, https://doi.org/10.1007/s11090-008-9132-4.

72. H. Uyama and O. Matsumoto, "Synthesis of Ammonia in High-Frequency Discharges. II. Synthesis of Ammonia in a Microwave Discharge Under Various Conditions," *Plasma Chemistry and Plasma Processing* 9 (1989): 421–432, https://doi.org/10.1007/BF01083676.

73. S. Dou, L. Tao, R. Wang, S. El Hankari, R. Chen, and S. Wang, "Plasma-Assisted Synthesis and Surface Modification of Electrode Materials for Renewable Energy," *Advanced Materials* 30 (2018): 1705850, https://doi.org/10.1002/adma.201705850.

74. K. Ollegott, P. Wirth, C. Oberste-Beulmann, P. Awakowicz, and M. Muhler, "Fundamental Properties and Applications of Dielectric Barrier Discharges in Plasma-Catalytic Processes at Atmospheric Pressure," *Chemie-Ingenieur-Technik* 92 (2020): 1542–1558, https://doi.org/10.1002/cite.202000075.

75. N. C. Roy, C. Pattyn, A. Remy, N. Maira, and F. Reniers, "NO_X Synthesis by Atmospheric-Pressure N_2/O_2 Filamentary DBD Plasma Over Water: Physicochemical Mechanisms of Plasma–Liquid Interactions," *Plasma Processes and Polymers* 18 (2020): 2000087, https://doi.org/10.1002/ppap.202000087.

76. U. Kogelschatz, "Dielectric-Barrier Discharges: Their History, Discharge Physics, and Industrial Applications," *Plasma Chemistry and Plasma Processing* 23 (2003): 1–46, https://doi.org/10.1023/A:1022470901385.

77. X. Tang, J. Wang, H. Yi, S. Zhao, F. Gao, and C. Chu, "Nitrogen Fixation and No Conversion Using Dielectric Barrier Discharge Reactor: Identification and Evolution of Products," *Plasma Chemistry and Plasma Processing* 38 (2018): 485–501, https://doi.org/10.1007/s11090-018-9876-4.

27662098, 2026, 1, Downloaded from https://onlinelibrary.wiley.com/doi/10.1002/EXP.20240438 by CochraneChina, Wiley Online Library on [08/06/2026]. See the Terms and Conditions (https://onlinelibrary.wiley.com/terms-and-conditions) on Wiley Online Library for rules of use; OA articles are governed by the applicable Creative Commons License

78. B. S. Patil, N. Cherkasov, N. V. Srinath, et al., "The Role of Heterogeneous Catalysts in the Plasma-Catalytic Ammonia Synthesis," *Catalysis Today* 362 (2021): 2–10, https://doi.org/10.1016/j.cattod.2020.06.074.

79. X. Zhu, J. Liu, X. Hu, et al., "Plasma-Catalytic Synthesis of Ammonia Over Ru-Based Catalysts: Insights Into the Support Effect," *Journal of the Energy Institute* 102 (2022): 240–246, https://doi.org/10.1016/j.joei.2022.02.014.

80. Y. Wang, M. Craven, X. Yu, et al., "Plasma-Enhanced Catalytic Synthesis of Ammonia Over a Ni/Al_2O_3 Catalyst at Near-Room Temperature: Insights Into the Importance of the Catalyst Surface on the Reaction Mechanism," *ACS Catalysis* 9 (2019): 10780–10793, https://doi.org/10.1021/acscatal.9b02538.

81. T. Mizushima, K. Matsumoto, H. Ohkita, and N. Kakuta, "Catalytic Effects of Metal-Loaded Membrane-Like Alumina Tubes on Ammonia Synthesis in Atmospheric Pressure Plasma by Dielectric Barrier Discharge," *Plasma Chemistry and Plasma Processing* 27 (2006): 1–11, https://doi.org/10.1007/s11090-006-9034-2.

82. A. Gómez-Ramírez, J. Cotrino, R. M. Lambert, and A. R. González-Elipe, "Efficient Synthesis of Ammonia From N2 and H2 Alone in a Ferroelectric Packed-Bed DBD Reactor," *Plasma Sources Science and Technology* 24 (2015): 065011.

83. K. van't Veer, Y. Engelmann, F. Reniers, and A. Bogaerts, "Plasma-Catalytic Ammonia Synthesis in a DBD Plasma: Role of Microdischarges and Their Afterglows," *Journal of Physical Chemistry C* 124 (2020): 22871–22883, https://doi.org/10.1021/acs.jpcc.0c05110.

84. P. Navascués, J. M. Obrero-Pérez, J. Cotrino, A. R. González-Elipe, and A. Gómez-Ramírez, "Unraveling Discharge and Surface Mechanisms in Plasma-Assisted Ammonia Reactions," *ACS Sustainable Chemistry & Engineering* 8 (2020): 14855–14866, https://doi.org/10.1021/acssuschemeng.0c04461.

85. P. Peng, P. Chen, M. Addy, et al., "Atmospheric Plasma-Assisted Ammonia Synthesis Enhanced via Synergistic Catalytic Absorption," *ACS Sustainable Chemistry Engineering* 7 (2018): 100–104, https://doi.org/10.1021/acssuschemeng.8b03887.

86. Y. Wang, W. Yang, S. Xu, et al., "Shielding Protection by Mesoporous Catalysts for Improving Plasma-Catalytic Ambient Ammonia Synthesis," *Journal of the American Chemical Society* 144 (2022): 12020–12031, https://doi.org/10.1021/jacs.2c01950.

87. B. Mindong, Z. Zhitao, B. Xiyao, B. Mindi, and N. Wang, "Plasma Synthesis of Ammonia With a Microgap Dielectric Barrier Discharge at Ambient Pressure," *IEEE Transactions on Plasma Science* 31 (2003): 1285–1291, https://doi.org/10.1109/TPS.2003.818761.

88. X. Pei, D. Gidon, and D. B. Graves, "Specific Energy Cost for Nitrogen Fixation as NO_X Using DC Glow Discharge in Air," *Journal of Physics D: Applied Physics* 53 (2019): 044002, https://doi.org/10.1088/1361-6463/ab5095.

89. J. J. Qiao, Q. Yang, D. Z. Wang, and Q. Xiong, "Energy Efficiency of N_2 Vibrational Excitation in the Spark-and-Glow Phases of a Long-Pulse Air Discharge at Atmospheric Pressure," *Plasma Sources Science and Technology* 32 (2023): 11LT01, https://doi.org/10.1088/1361-6595/ad08f6.

90. C. Wildfire, V. Abdelsayed, D. Shekhawat, and M. J. Spencer, "Ambient Pressure Synthesis of Ammonia Using a Microwave Reactor," *Catalysis Communications* 115 (2018): 64–67, https://doi.org/10.1016/j.catcom.2018.07.010.

91. S. Kelly and A. Bogaerts, "Nitrogen Fixation in an Electrode-Free Microwave Plasma," *Joule* 5 (2021): 3006–3030, https://doi.org/10.1016/j.joule.2021.09.009.

92. A. Indarto, D. R. Yang, J. W. Choi, H. Lee, and H. K. Song, "Gliding Arc Plasma Processing of CO_2 Conversion," *Journal of Hazardous Materials* 146 (2007): 309–315, https://doi.org/10.1016/j.jhazmat.2006.12.023.

93. G. Petitpas, J. Rollier, A. Darmon, J. Gonzalezaguilar, R. Metkemeijer, and L. Fulcheri, "A Comparative Study of Non-Thermal Plasma Assisted Reforming Technologies," *International Journal of Hydrogen Energy* 32 (2007): 2848–2867, https://doi.org/10.1016/j.ijhydene.2007.03.026.

94. H. Chen, A. Wu, S. Mathieu, et al., "Highly Efficient Nitrogen Fixation Enabled by an Atmospheric Pressure Rotating Gliding Arc," *Plasma Processes and Polymers* 18 (2021): 2000200, https://doi.org/10.1002/ppap.202000200.

95. F. Zhu, H. Zhang, X. Li, et al., "Arc Dynamics of a Pulsed DC Nitrogen Rotating Gliding Arc Discharge," *Journal of Physics D: Applied Physics* 51 (2018): 105202, https://doi.org/10.1088/1361-6463/aaa9eb.

96. Y. Luo, H. Jiang, L. X. Ding, et al., "Selective Synthesis of either Nitric Acid or Ammonia From Air by Electrolyte Regulation in a Plasma Electrolytic System," *ACS Sustainable Chemistry & Engineering* 11 (2023): 11737–11744, https://doi.org/10.1021/acssuschemeng.2c06506.

97. J. Zhan, A. Zhang, P. Héroux, et al., "Gasoline Degradation and Nitrogen Fixation in Soil by Pulsed Corona Discharge Plasma," *Science of the Total Environment* 661 (2019): 266–275, https://doi.org/10.1016/j.scitotenv.2019.01.183.

98. S. R. Noh, D. S. Kim, S. J. Park, and M. Choi, "Enhanced Yield of Positively Charged Particles From a Spark Discharge Generator via In Situ Corona Discharges," *Journal of Aerosol Science* 101 (2016): 188–195, https://doi.org/10.1016/j.jaerosci.2016.08.003.

99. R. K. Sharma, H. Patel, U. Mushtaq, et al., "Plasma Activated Electrochemical Ammonia Synthesis From Nitrogen and Water," *ACS Energy Letters* 6 (2020): 313–319, https://doi.org/10.1021/acsenergylett.0c02349.

100. W. Li, S. Zhang, J. Ding, et al., "Sustainable Nitrogen Fixation to Produce Ammonia by Electroreduction of Plasma-Generated Nitrite," *ACS Sustainable Chemistry & Engineering* 11 (2023): 1168–1177, https://doi.org/10.1021/acssuschemeng.2c06525.

101. W. Liu, M. Xia, C. Zhao, et al., "Efficient Ammonia Synthesis From the Air Using Tandem Non-Thermal Plasma and Electrocatalysis at Ambient Conditions," *Nature Communications* 15 (2024): 3524, https://doi.org/10.1038/s41467-024-47765-9.

102. Z. Meng, J. X. Yao, C. N. Sun, et al., "Efficient Ammonia Production Beginning From Enhanced Air Activation," *Advanced Energy Materials* 12 (2022): 2202105, https://doi.org/10.1002/aenm.202202105.

103. Y. Liu, J. Ma, S. Huang, S. Niu, and S. Gao, "Highly Dispersed Copper-Iron Nanoalloy Enhanced Electrocatalytic Reduction Coupled With Plasma Oxidation for Ammonia Synthesis From Ubiquitous Air and Water," *Nano Energy* 117 (2023): 108840, https://doi.org/10.1016/j.nanoen.2023.108840.

104. J. Sun, D. Alam, R. Daiyan, et al., "A Hybrid Plasma Electrocatalytic Process for Sustainable Ammonia Production," *Energy & Environmental Science* 14 (2021): 865–872, https://doi.org/10.1039/D0EE03769A.

105. T. Haruyama, T. Namise, N. Shimoshimizu, et al., "Non-Catalyzed One-Step Synthesis of Ammonia From Atmospheric Air and Water," *Green Chemistry* 18 (2016): 4536–4541, https://doi.org/10.1039/C6GC01560C.

106. P. Lamichhane, B. C. Adhikari, L. N. Nguyen, et al., "Sustainable Nitrogen Fixation From Synergistic Effect of Photo-Electrochemical Water Splitting and Atmospheric Pressure N_2 Plasma," *Plasma Sources Science and Technology* 29 (2020): 045026, https://doi.org/10.1088/1361-6595/ab7f4d.

107. P. Peng, P. Chen, M. Addy, et al., "In Situ Plasma-Assisted Atmospheric Nitrogen Fixation Using Water and Spray-Type Jet Plasma," *Chemical Communications* 54 (2018): 2886–2889, https://doi.org/10.1039/C8CC00697K.

108. T. Sakakura, N. Murakami, Y. Takatsuji, M. Morimoto, and T. Haruyama, "Contribution of Discharge Excited Atomic N, N_2 *, and N_2+ to a Plasma/Liquid Interfacial Reaction as Suggested by Quantitative Analysis," *Chemphyschem* 20 (2019): 1467–1474, https://doi.org/10.1002/cphc.201900212.

109. J. A. Andersen, M. C. Holm, K. van't Veer, et al., "Plasma-Catalytic Ammonia Synthesis in a Dielectric Barrier Discharge Reactor: A Combined Experimental Study and Kinetic Modeling," *Chemical Engineering Journal* 457 (2023): 141294, https://doi.org/10.1016/j.cej.2023.141294.

27662098, 2026, 1, Downloaded from https://onlinelibrary.wiley.com/doi/10.1002/EXP.20240438 by CochraneChina, Wiley Online Library on [08/06/2026]. See the Terms and Conditions (https://onlinelibrary.wiley.com/terms-and-conditions) on Wiley Online Library for rules of use; OA articles are governed by the applicable Creative Commons License

110. T. Wu, B. Chang, Y. Li, et al., "Laser-Induced Plasma and Local Temperature Field for High-Efficiency Ammonia Synthesis," *Nano Energy* 116 (2023): 108855, https://doi.org/10.1016/j.nanoen.2023.108855.

111. X. Hu, S. Zhang, L. Dou, Y. Gao, C. Zhang, and T. Shao, "Plasma-Enabled Sustainable Ammonia Synthesis at Atmospheric Pressure: The Role of Catalysts on Synergistic Effect," *Catalysis Today* 422 (2023): 114245, https://doi.org/10.1016/j.cattod.2023.114245.

112. I. Muzammil, Y. N. Kim, H. Kang, et al., "Plasma Catalyst-Integrated System for Ammonia Production From H_2O and N_2 at Atmospheric Pressure," *ACS Energy Letters* 6 (2021): 3004–3010, https://doi.org/10.1021/acsenergylett.1c01497.

113. M. M. Shi, D. Bao, B. R. Wulan, et al., "Au Sub-Nanoclusters on TiO_2 Toward Highly Efficient and Selective Electrocatalyst for N_2 Conversion to NH_3 at Ambient Conditions," *Advanced Materials* 29 (2017): 1606550, https://doi.org/10.1002/adma.201606550.

114. X. Zhang, Q. Liu, X. Shi, et al., "TiO_2 Nanoparticles–reduced Graphene Oxide Hybrid: An Efficient and Durable Electrocatalyst Toward Artificial N_2 Fixation to NH_3 Under Ambient Conditions," *Journal of Materials Chemistry A* 6 (2018): 17303–17306, https://doi.org/10.1039/C8TA05627G.

115. H. Tao, C. Choi, L. X. Ding, et al., "Nitrogen Fixation by Ru Single-Atom Electrocatalytic Reduction," *Chemistry* 5 (2019): 204–214, https://doi.org/10.1016/j.chempr.2018.10.007.

116. Y. Zhang, W. Qiu, Y. Ma, et al., "High-Performance Electrohydrogenation of N_2 to NH_3 Catalyzed by Multishelled Hollow Cr_2O_3 Microspheres Under Ambient Conditions," *ACS Catalysis* 8 (2018): 8540–8544, https://doi.org/10.1021/acscatal.8b02311.

117. W. Qiu, X. Y. Xie, J. Qiu, et al., "High-Performance Artificial Nitrogen Fixation at Ambient Conditions Using a Metal-Free Electrocatalyst," *Nature Communications* 9 (2018): 3485, https://doi.org/10.1038/s41467-018-05758-5.

118. Y. Zhao, Y. Zhao, G. I. N. Waterhouse, et al., "Layered-Double-Hydroxide Nanosheets as Efficient Visible-Light-Driven Photocatalysts for Dinitrogen Fixation," *Advanced Materials* 29 (2017): 1703828, https://doi.org/10.1002/adma.201703828.

119. G. Dong, W. Ho, and C. Wang, "Selective Photocatalytic N_2 Fixation Dependent on G-C_3N_4 Induced by Nitrogen Vacancies," *Journal of Materials Chemistry A* 3 (2015): 23435–23441, https://doi.org/10.1039/C5TA06540B.

120. S. Wang, X. Hai, X. Ding, et al., "Photocatalysis: Light-Switchable Oxygen Vacancies in Ultrafine Bi_5O_7Br Nanotubes for Boosting Solar-Driven Nitrogen Fixation in Pure Water (Adv. Mater. 31/2017)," *Advanced Materials* 29 (2017): 31.

121. H. Li, J. Shang, J. Shi, K. Zhao, and L. Zhang, "Facet-Dependent Solar Ammonia Synthesis of BiOCl Nanosheets via a Proton-Assisted Electron Transfer Pathway," *Nanoscale* 8 (2016): 1986–1993, https://doi.org/10.1039/C5NR07380D.

122. S. Sun, X. Li, W. Wang, L. Zhang, and X. Sun, "Photocatalytic Robust Solar Energy Reduction of Dinitrogen to Ammonia on Ultrathin MoS_2," *Applied Catalysis B* 200 (2017): 323–329, https://doi.org/10.1016/j.apcatb.2016.07.025.

123. M. Kitano, J. Kujirai, K. Ogasawara, et al., "Low-Temperature Synthesis of Perovskite Oxynitride-Hydrides as Ammonia Synthesis Catalysts," *Journal of the American Chemical Society* 141 (2019): 20344–20353, https://doi.org/10.1021/jacs.9b10726.

124. Y. Inoue, M. Kitano, K. Kishida, et al., "Efficient and Stable Ammonia Synthesis by Self-Organized Flat Ru Nanoparticles on Calcium Amide," *ACS Catalysis* 6 (2016): 7577–7584, https://doi.org/10.1021/acscatal.6b01940.

125. F. Chang, Y. Guan, X. Chang, et al., "Alkali and Alkaline Earth Hydrides-Driven N_2 Activation and Transformation Over Mn Nitride Catalyst," *Journal of the American Chemical Society* 140 (2018): 14799–14806, https://doi.org/10.1021/jacs.8b08334.

126. P. Wang, F. Chang, W. Gao, et al., "Breaking Scaling Relations to Achieve Low-Temperature Ammonia Synthesis Through LiH-Mediated Nitrogen Transfer and Hydrogenation," *Nature Chemistry* 9 (2016): 64–70, https://doi.org/10.1038/nchem.2595.

127. Z. Wang, J. Lin, R. Wang, and K. Wei, "Ammonia Synthesis Over Ruthenium Catalyst Supported on Perovskite Type $BaTiO_3$," *Catalysis Communications* 32 (2013): 11–14, https://doi.org/10.1016/j.catcom.2012.11.024.

128. J. Zheng, H. Zhang, J. Lv, et al., "Enhanced NH_3 Synthesis From Air in a Plasma Tandem-Electrocatalysis System Using Plasma-Engraved N-Doped Defective MoS_2," *JACS Au* 3 (2023): 1328–1336, https://doi.org/10.1021/jacsau.3c00087.

129. A. Wu, J. Yang, B. Xu, et al., "Direct Ammonia Synthesis From the Air via Gliding Arc Plasma Integrated With Single Atom Electrocatalysis," *Applied Catalysis B* 299 (2021): 120667, https://doi.org/10.1016/j.apcatb.2021.120667.

130. J. Ding, W. Li, Q. Chen, et al., "Sustainable Ammonia Synthesis From Air by the Integration of Plasma and Electrocatalysis Techniques," *Inorganic Chemistry Frontiers* 10 (2023): 5762–5771, https://doi.org/10.1039/D3QI00915G.

131. H. Ma, R. K. Sharma, S. Welzel, M. C. Van de Sanden, M. N. Tsampas, and W. F. Schneider, "Observation and Rationalization of Nitrogen Oxidation Enabled Only by Coupled Plasma and Catalyst," *Nature Communications* 13 (2022): 402, https://doi.org/10.1038/s41467-021-27912-2.

132. B. Luo, X. Liu, K. Ma, et al., "Plasma-Driven NH_3 Synthesis From N_2 and H_2O Over Ni-Co/CeO_x With Nearly 100% Selectivity," *Applied Catalysis B* 379 (2025): 125677, https://doi.org/10.1016/j.apcatb.2025.125677.

133. Y. Gong, P. Lamichhane, M. Walker, V. Hessel, and E. Rebrov, "Enhanced Ammonia Production Through Non-Thermal Plasma-Assisted Synthesis: Tailoring Titanium Oxynitride Photocatalysts for Optimal Performance," *Chemical Engineering Journal* 519 (2025): 165118, https://doi.org/10.1016/j.cej.2025.165118.

134. B. Lu, S. Sun, and H. Qiu, "Exploring the Origin of Synergistic Effect in Plasma-Assisted Ammonia Synthesis Over a Ni Catalyst," *Langmuir* 41 (2025): 13119–13125, https://doi.org/10.1021/acs.langmuir.5c00745.

135. K. H. R. Rouwenhorst, F. Jardali, A. Bogaerts, and L. Lefferts, "From the Birkeland–Eyde Process Towards Energy-Efficient Plasma-Based NO_X Synthesis: A Techno-Economic Analysis," *Energy & Environmental Science* 14 (2021): 2520–2534, https://doi.org/10.1039/D0EE03763J.

136. D. K. Dinh, I. Muzammil, W. S. Kang, D. Kim, and D. H. Lee, "Reducing Energy Cost of In Situ Nitrogen Fixation in Water Using an Arc-DBD Combination," *Plasma Sources Science and Technology* 30 (2021): 055020, https://doi.org/10.1088/1361-6595/abff72.

137. G. Xu, R. Liu, and J. Wang, "Electrochemical Synthesis of Ammonia Using a Cell With a Nafion Membrane and $SmFe_{0.7}Cu_{0.3-x}$ Ni_x O_3 (x = 0−0.3) Cathode at Atmospheric Pressure and Lower Temperature," *Science in China Series B-Chemistry* 52 (2009): 1171–1175, https://doi.org/10.1007/s11426-009-0135-7.

138. R. Lan and S. Tao, "Electrochemical Synthesis of Ammonia Directly From Air and Water Using a $Li^+/H^+/NH_4^+$ Mixed Conducting Electrolyte," *RSC Advances* 3 (2013): 18016, https://doi.org/10.1039/c3ra43432j.

139. J. N. Renner, L. F. Greenlee, K. E. Ayres, and A. M. Herring, "Electrochemical Synthesis of Ammonia: A Low Pressure, Low Temperature Approach," *Electrochemical Society Interface* 24 (2015): 51–57, https://doi.org/10.1149/2.F04152if.

140. H. H. Kim, Y. Teramoto, A. Ogata, H. Takagi, and T. Nanba, "Atmospheric-Pressure Nonthermal Plasma Synthesis of Ammonia Over Ruthenium Catalysts," *Plasma Processes and Polymers* 14 (2016): 1600157, https://doi.org/10.1002/ppap.201600157.

141. W. P. Liang, X. M. Zhang, P. W. Bai, et al., "Cascade N_2 Reduction Process With DBD Plasma Oxidation and Electrocatalytic Reduction for Continuous Ammonia Synthesis," *Environmental Science & Technology* 57 (2023): 14558–14568, https://doi.org/10.1021/acs.est.3c05443.

27662098, 2026, 1, Downloaded from https://onlinelibrary.wiley.com/doi/10.1002/EXP.20240438 by CochraneChina, Wiley Online Library on [08/06/2026]. See the Terms and Conditions (https://onlinelibrary.wiley.com/terms-and-conditions) on Wiley Online Library for rules of use; OA articles are governed by the applicable Creative Commons License

142. H. Chen, D. Yuan, A. Wu, X. Lin, and X. Li, "Review of Low-Temperature Plasma Nitrogen Fixation Technology," *Waste Disposal & Sustainable Energy* 3 (2021): 201–217, https://doi.org/10.1007/s42768-021-00074-z.

143. Y. Ma, Y. Tian, Y. Zeng, and X. Tu, "Plasma Synthesis of Ammonia in a Tangled Wire Dielectric Barrier Discharge Reactor: Effect of Electrode Materials," *Journal of the Energy Institute* 99 (2021): 137–144, https://doi.org/10.1016/j.joei.2021.09.002.

144. J. Shah, W. Wang, A. Bogaerts, and M. L. Carreon, "Ammonia Synthesis by Radio Frequency Plasma Catalysis: Revealing the Underlying Mechanisms," *ACS Applied Energy Materials* 1 (2018): 4824–4839, https://doi.org/10.1021/acsaem.8b00898.

145. R. Hawtof, S. Ghosh, E. Guarr, C. Xu, R. Mohan Sankaran, and J. N. Renner, "Catalyst-Free, Highly Selective Synthesis of Ammonia From Nitrogen and Water by a Plasma Electrolytic System," *Science Advances* 5 (2019): eaat5778, https://doi.org/10.1126/sciadv.aat5778.

27662098, 2026, 1, Downloaded from https://onlinelibrary.wiley.com/doi/10.1002/EXP.20240438 by CochraneChina, Wiley Online Library on [08/06/2026]. See the Terms and Conditions (https://onlinelibrary.wiley.com/terms-and-conditions) on Wiley Online Library for rules of use; OA articles are governed by the applicable Creative Commons License